**Master's Thesis of Science in Agriculture**

# Pathogenic and Molecular Characterization of the Interactions between Broad Bean Wilt Virus 2 and Its Hosts

잠두위조바이러스 2 와 기주 간의

병원성 및 분자적 상호작용에 대한 특성 구명

**August 2021**

**Myung-Hwi Kim**

**Department of International Agricultural Technology**

**Graduate School of International Agricultural Technology**

**Seoul National University**

# Pathogenic and Molecular Characterization of the Interactions between Broad Bean Wilt Virus 2 and Its Hosts

A thesis
submitted in partial fulfillment of the requirements to the faculty
of Graduate School of International Agricultural Technology
for the Degree of Master of Science in Agriculture

By
Myung-Hwi Kim

Supervised by
Prof. Jang-Kyun Seo

Major of Crop Biotechnology
Department of International Agricultural Technology
Graduate School of International Agricultural Technology
Seoul National University

August 2021

Approved as a qualified thesis
for the Degree of Master of Science in Agriculture
by the committee members

**Chairman** **Jin-Ho Kang, Ph.D.**

**Member** **Ju-Kon Kim, Ph.D.**

**Member** **Jang-Kyun Seo, Ph.D.**

# ABSTRACT

## Pathogenic and Molecular Characterization of the Interactions between Broad Bean Wilt Virus 2 and Its Hosts

**Myung-Hwi Kim**

**Major of Crop Biotechnology**

**Department of International Agricultural Technology**

**Graduate School of International Agricultural Technology**

**Seoul National University**

Broad bean wilt virus 2 (BBWV2; genus *Fabavirus*, family *Secoviridae*) is an evolutionary successful RNA virus since it has an extensive host range and has spread worldwide. Numerous BBWV2 isolates have been identified and genomic sequenced from various plant species, but little information is available on the virulence and symptomatic characteristics associated with a genomic sequence, and molecular properties for interactions with host proteins. In this study, we provide integrated information for molecular and pathogenic

characteristics of three genetically distant BBWV2 isolates: BBWV2-PC, -LS2, and P3 obtained from different host species, respectively, as well as evidence for host proteins that will interact with the movement protein of BBWV2 to be involved in viral movement. Phylogenetic and diversity analyses of the BBWV2 population including 42 isolates from various host species revealed that RNA2 has higher genetic plasticity than RNA1 and may have evolved under host-imposed constraints. In addition, we generated an infectious cDNA clone of BBWV2-PC RNA2 (pBBWV2-PC-R2). Pseudo-recombination analysis of pBBWV2-PC-R2 further demonstrated that RNA2 contains a viral factor(s) associated with pathogenic diversification of BBWV2. Plant viruses are obligate parasites and require various host factors during their life cycle, including genomic replication and cell-to-cell and systemic movement. In particular, viruses move from an initially infected cell to neighboring cells through plasmodesmata (PD) for successful infection. In this process, viral movement proteins (MPs) interact with various host factors and function to facilitate intercellular movement of viral RNAs and to increase the size exclusion limit of PD. In BBWV2, VP37 encoded in RNA2 functions as a MP. In this study, we identified heat-shock protein 90 (Hsp90) as a host factor interacting with VP37 through co-immunoprecipitation. Hsp90 is a molecular chaperone that maintains the genetic homeostasis of plants by interacting with several co-chaperones in various biological processes. Yeast two-hybrid assay (Y2H) demonstrated the direct interaction between VP37 and Hsp90. We further analyzed the VP37/Hsp90 interaction based on Y2H to identify crucial motifs and amino acid residues for this interaction. We identified two amino acid residues (E5 and E12) in the N-terminal region of Hsp90 crucial for the interaction with VP37. Therefore, our study suggests that RNA2 and its encoding proteins are highly associated with the BBWV2-host interactions that determine the pathogenic and biological characteristics of the virus.

……

**Keywords: Broad bean wilt virus 2, Population diversity, Pathogenicity, Host-virus interaction, Protein-protein interaction**

***Student Number*: 2019-27060**

# CONTENTS

# LIST OF TABLES

**Chapter 1**

**Genetic plasticity in RNA2 is associated with pathogenic diversification of broad bean wilt virus 2**



**Chapter 2**

**Molecular characterization of the interactions between broad bean wilt virus 2 VP37 and heat shock protein 90**

# LIST OF FIGURES

**Chapter 1**

**Genetic plasticity in RNA2 is associated with pathogenic diversification of broad bean wilt virus 2**



**Chapter 2**

**Molecular characterization of the interactions between broad bean wilt virus 2 37 and heat shock protein 90**

# Chapter 1

# Genetic plasticity in RNA2 is associated with pathogenic diversification of broad bean wilt virus 2

# INTRODUCTION

Broad bean wilt virus 2 (BBWV2; genus *Fabavirus*, family *Secoviridae*) is an evolutionary successful RNA virus. It has a wide host range, is easily transmitted by aphid vectors, and damages various agriculturally important crops worldwide (Ferrer et al. 2011; Kwak et al. 2013a). Accordingly, many BBWV2 isolates have been identified from various hosts and their partial or complete genomes sequences have been determined (Ferrer et al. 2011; Kwak et al. 2013a). BBWV2 causes diverse symptoms, including mosaic, mottling, necrosis, wilting, and stunting, depending on the compatibility between virus isolates and host plants (Kwak et al. 2013a; Kwak et al. 2013b). Symptomatic variation in a host plant when infected with different virus strains is the result of specific interactions between host and viral factors. A strain-specific viral protein can function as the specific elicitor determining the symptomatic phenotype of viral disease (Seo et al. 2009). Therefore, in general, genetically distant viral strains also differ in pathogenicity.

The BBWV2 genome is composed of two single-stranded, positive-sense RNAs, RNA1 (≅5.8 kb) and RNA2 (≅3.3 kb), which are encapsulated separately into icosahedral virions (Ferrer et al. 2011). The 5' end of each RNA is linked to viral genome-linked protein (VPg), and the 3' end is polyadenylated. Each RNA segment contains a single open reading frame (ORF) that is translated into one large single polyprotein precursor. The polyprotein precursor encoded by RNA1 is processed by proteolytic cleavage to yield five mature proteins: protease cofactor (Co-Pro), NTP-binding motif (NTBM), VPg, protease (Pro), and RNA-dependent RNA polymerase (RdRp). Also, the polyprotein precursor encoded by RNA2 is processed to yield three mature proteins: movement protein (MP), large coat protein (LCP), and small coat protein (SCP) (Ferrer et al. 2011; Kwak et al. 2013a).

Availability of both genetic and pathogenic information of virus isolates is essential for identifying viral factors associated with pathogenicity. Recently, infectious cDNA clones of two BBWV2 strains, RP1 and PAP1 isolated from pepper, were generated, and their pathogenic characteristics were examined (Kwak et al. 2016). Integrated analysis of genetic and pathogenic characteristics of the strains RP1 and PAP1 resulted in the identification of MP as a viral determinant of symptom severity (Seo et al. 2017). In our previous studies, we obtained various BBWV2 isolates from several plant species and determined their complete genome sequences (Kwak et al. 2013a; Kwak et al. 2013b; Seo et al. 2014). In this study, we provide detailed phylogenetic and pathogenic information on three genetically distant BBWV2 isolates, PC, LS2, and P3 from *Gentiana scabra*, *Leonurus sibiricus*, and *Pisum sativum*, respectively, based on in-depth analysis of their molecular and biological characteristics.

# MATERIALS AND METHODS

## 1. Phylogenetic tree analysis

Phylogenetic analysis was carried out with amino acid sequences of the full length of BBWV2-RNA1, BBWV2-RNA2 ORF region were compared with 42 BBWV2 isolates and one broad bean wilt virus 1 (BBWV1-PV132) as an outgroup taxon [GenBank accession numbers for BBWV1-PV132: NC_005289 (RNA1) and NC_005290 (RNA2)] registered in NCBI; these included all BBWV2 isolates for which a complete genome sequence was currently available (Table 1). Amino acid sequence alignment was performed using ClustalW implemented in MEGA X software (Kumar et al. 2018) and the phylogenetic tree were reconstructed by the maximum-likelihood method (Jones-Taylor-Thornton-model) in MEGA X with bootstrap values calculated using 1,000 random-replications.

**Table 1.** BBWV2 isolates and strains analyzed in this study

| Isolate or strain | Collecting host | Country of origin | Collection year | Accession number | |
|---|---|---|---|---|---|
| | | | | RNA1 | RNA2 |
| AB1 | *Achyranthes bidentata* | Korea | 2017 | MH447988 | MH447989 |
| Am | *Atractylodes macrocephala* | China | 2011 | JX575182 | KC110085 |
| Anhui | *Vicia faba* | China | 2015 | KY606992 | KY606993 |
| BB2 | *Vicia faba* | Korea | 2006 | KC625492 | KC625506 |
| BB5 | *Vicia faba* | Korea | 2006 | KC625493 | KC625507 |
| BB9 | *Vicia faba* | Korea | 2006 | KC625494 | KC625508 |
| BR | *Dioscorea oppositifolia* | Korea | 2015 | KX234809 | KX234810 |
| BRI | *Dioscorea oppositifolia* | Korea | 2015 | KU641565 | KU309314 |
| Ca | *Capsicum annuum* | China | 2012 | KF498696 | KF498697 |
| DO | *Dioscorea opposita* | Korea | 2015 | KT246495 | KT246496 |
| GP2 | *Capsicum annuum* var. gulosum | Korea | 212 | KC625495 | KC625509 |
| GP4 | *Capsicum annuum* var. gulosum | Korea | 2012 | KC625496 | KC625510 |
| GP5 | *Capsicum annuum* var. gulosum | Korea | 2012 | KC625497 | KC625511 |
| Hunan | *Capsicum annuum* | China | 2013 | KJ789403 | KJ825857 |
| IA | *Gentiana* spp | Japan | Unknown | AB051386 | AB032403 |
| IP | *Capsicum annuum* | Japan | Unknown | AB023484 | AB018698 |
| LN | *Sesamum indicum* | China | 2017 | MK116519 | MK118749 |
| LNSY | *Chenopodium album* | China | 2016 | MN786954 | MN786955 |
| LS2 | *Leonurus sibiricus* | Korea | 2012 | KM076648 | KM076649 |
| MB7 | *Vicia faba* | Japan | Unknown | AB013615 | AB013616 |
| ME | *Megaskepasma erythrochlamys* | Singapore | 1991 | NC_003003 | NC_003004 |
| P2 | *Pisum sativum* | Korea | 2007 | KC625498 | KC625512 |
| P3 | *Pisum sativum* | Korea | 2007 | KC625499 | KC625513 |
| PAP1 | *Capsicum annuum* var. gulosum | Korea | 2010 | KT380020 | KT380021 |
| PAP2 | *Capsicum annuum* var. gulosum | Korea | 2010 | KC625501 | KC625514 |
| PAP3 | *Capsicum annuum* var. gulosum | Korea | 2011 | KC625502 | KC625515 |
| PC | *Gentiana scabra* | Korea | 2017 | MW939476 | MW939477 |
| RP1 | *Capsicum annuum* | Korea | 2007 | KT380022 | KT380023 |
| RP2 | *Capsicum annuum* | Korea | 2007 | JX183223 | JX183224 |
| RP3 | *Capsicum annuum* | Korea | 2007 | JX183225 | JX183226 |
| RP4 | *Capsicum annuum* | Korea | 2007 | JX183227 | JX183228 |
| RP5 | *Capsicum annuum* | Korea | 2009 | JX183229 | JX183230 |
| RP6 | *Capsicum annuum* | Korea | 2010 | JX183231 | JX183232 |
| RP7 | *Capsicum annuum* | Korea | 2011 | JX183233 | JX183234 |
| SG1 | *Dioscorea opposita* | China | 2011 | KJ789136 | KJ789137 |
| SN | *Gynura procumbens* | Korea | 2015 | KX686589 | KX686590 |
| SP | *Spinacia oleracea* | Korea | 2007 | KC625505 | KC625518 |
| SP1 | *Spinacia oleracea* | Korea | 2007 | KC625503 | KC625516 |
| SP2 | *Spinacia oleracea* | Korea | 2007 | KC625504 | KC625517 |
| Ty | *Gentiana triflora* | Japan | Unknown | AB746938 | AB746939 |
| XJ14-3 | *Solanum lycopersicum* | China | Unknown | FN985164 | HQ283389 |
| XJP1-1 | *Capsicum annuum* | China | 2012 | KC790225 | HQ283390 |

**2. Comparative amino acid diversity analysis**

Amino acid diversity analysis was performed using 42 isolates; these included all BBWV2 isolates (Table 1). The genetic diversities within and between groups in the phylogeny of each RNA segment were estimated by Poisson model in MEGA X (Kumar et al. 2018).

**3. Comparative nucleotide diversity analysis**

The nucleotide diversity estimated by the maximum composite likelihood method in MEGA X software (Kumar et al. 2018). Pairwise genetic differences at nonsynonymous (*d*N) and synonymous (*d*S) nucleotide positions for each cistronic region using the Nei-Gojobori method in MEGA X, respectively (Kumar et al. 2018).

**4. Mechanical inoculation and virus detection**

Three isolates, PC, LS2, and P3, from our BBWV2 collection to investigate their pathogenicity in various plant species. BBWV2 strain RP1 was included in the inoculation experiments as a reference strain since its pathogenicity was well characterized (Kwak et al. 2016). Each BBWV2 variant was isolated by serial mechanical transmission in *Chenopodium quinoa* and propagated in *Nicotiana benthamiana*. Crude sap was prepared from symptomatic leaves of *N. benthamiana* infected with each isolate and mechanically inoculated on the leaves of various plant species. The inoculated plants were grown in an insect-free growth chamber (26°C during the day and 24°C at night with a 16-h photoperiod) and monitored for at least 25 days post-inoculation (dpi) to analyze symptomatology. RT-PCR detection was performed using specific primers (5'-AAACAAACAGCTTTCGTTCCG-3' and 5'-GCCATCTCATTG GCATGGA-3') to confirm systemic viral infection at 20 dpi, as described previously (Kwak et al. 2013b).

**5. Infectivity test of pseudo recombinant clones**

Infectious cDNA clone of BBWV2-PC-RNA2 construct was generated based on a modified binary vector, pCass-Rz vector as previously described (Choi et al. 2019; de Wispelaere and Rao. 2009; Kwak et al. 2016). The resulting construct was designated pBBWV2-PC-R2 (Figure. 1). The cDNA infectious clones of BBWV2 were individually transformed into *Agrobacterium tumefaciens* strain EHA105 by freeze-thaw lysis method. Cells of *A. tumefaciens* harboring each chimeric RNA2 construct were grown in LB media containing kanamycin (100 ug/ml), rifampicin (50 ug/ml) at 28°C for overnight. Infectious cDNA clones of RNA1 and RNA2 of BBWV2 strain RP1 (pBBWV2-RP1-R1 and -R2, respectively) were obtained from our previous study and were cultured together (Kwak et al. 2016). All Agrobacteruim transformants were resuspended to $OD_{600}$ of 0.7 with infiltration buffer (10 mM MES, 10 mM $MgCl_2$, and 200 μM acetosyringone, pH 5.6). And mixed equal proportions with cells of *A. tumefaciens* harboring pBBWV2-RP1-R1 for agroinfiltration (Kwak et al., 2016). Resuspended cultures were incubated at 28°C shaking incubator for 4 hours. Each mixture was infiltrated into the abaxial surface of the leaves of *N. benthamiana*. Symptoms development was monitored for 21 day post-inoculation and BBWV2 infection was confirmed by RT-PCR using total RNA extracted from upper non-inoculated leaves and the suitable primer pairs (5'-TTCGGATGTGACCATGGCTGGTGCATT-3' and 5'-GACCTAGGTTGGCCATATCTATAATCCTTGC-3').

Each pseudo recombinant clones crude sap was prepared from symptomatic leaves of *N. benthamiana* infected with each isolate and mechanically inoculated on the leaves of various plant species; *N. occidentalis*, *Capsicum spp*., *Cucumis sativus*, *Chenopodium spp*., *Perilla frutescens*, *P. sativum*, *Solanum lycopersicum*, *Spinacia oleracea*, *Vicia faba*. All plants were grown in a growth chamber under 16 h/24°C day and 8 h/20°C night conditions except *S. oleracea*. The *S. oleracea* was grown in a growth chamber under 16 h/30°C

day and 8 h/25°C night conditions. All plants monitored for at least 14 to 35 days post-inoculation to analyze symptomatology. In all plants total RNA were extracted using Hybrid-R$^{TM}$ (GeneAll, Korea) and cDNA synthesized using M-MulV Reverse Transcriptase (NEB, USA) with reverse primer (5'-TGGAG GCTAGTGACCTAC-3') and RT-PCR detection was performed using specific primers (5'- TGGCTGAATGCTCCGAAAGT-3' and 5'- AATTCGCCACTTG GACTCGT-3') to confirm systemic viral infection at 14 dpi.

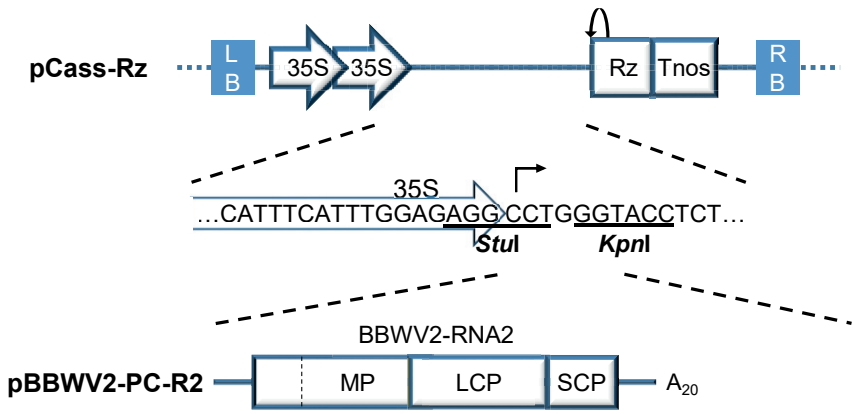


**Figure 1.** Schematic representation of the full-length cDNA clone of BBWV2-PC RNA2. Full-length cDNA of RNA2 was inserted between the *Stu*I and *Kpn*I sites in the pCass-Rz vector. The pCassRz vector contains, in sequential order, a T-DNA left border (LB), a double 35S promoter, cloning sites (*Stu*I and *Kpn*I), a cis-cleaving ribozyme sequence (Rz), a 35S terminator (T), and a T-DNA right border (RB). Transcription begins at the first nucleotide of the cDNA.

## 6. Amino acid comparison of infectious cDNA clones

Amino acid alignment in RNA2 of the infectious cDNA clone of BBWV2-RP1 and -PC was performed using ClustalW implemented in MEGA X software (Kumar et al. 2018).

# RESULT

## 1. Phylogenetic structure of the BBWV2 population

To examine the evolutionary relationships we performed phylogenetic analyses on 42 isolates. The phylogenetic trees showed that the genetic divergence of the BBWV2 population showed different patterns for each RNA segment (Figure. 2). The polyprotein amino acid sequences encoded by RNA1, the BBWV2 isolates were clearly split into two main groups: group A consisted mainly of the BBWV2 isolates from pepper, while group B included various isolates from different hosts (Figure. 2A). The polyprotein amino acid sequences encoded by RNA2, an obvious cluster consisting mainly of the isolates from pepper was also formed (Figure. 2B; group A). However, the degree of divergence (i.e. branch length) among the remaining viral isolates (Figure. 2B; group B) was significantly higher in the RNA2 phylogeny than that found in group B in the RNA1 phylogeny (Figure. 2A).

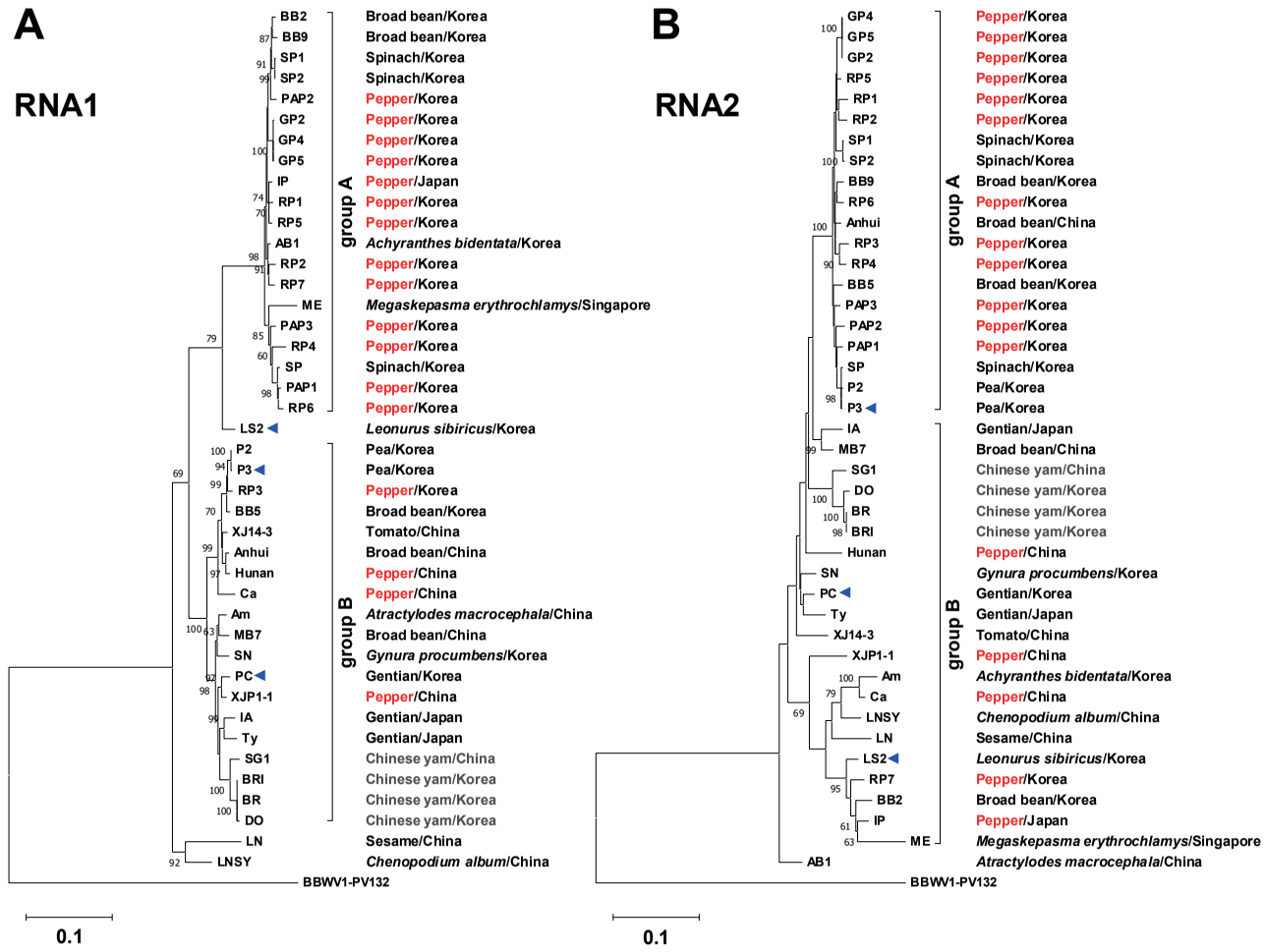
A
RNA1
BB2 Broad bean/Korea
BB9 Broad bean/Korea
SP1 Spinach/Korea
SP2 Spinach/Korea
PAP2 Pepper/Korea
GP2 Pepper/Korea
GP4 Pepper/Korea
GP5 Pepper/Korea
IP Pepper/Japan
RP1 Pepper/Korea
RP5 Pepper/Korea
AB1 Achyranthes bidentata/Korea
RP2 Pepper/Korea
RP7 Pepper/Korea
ME Megaskepasma erythrochlamys/Singapore
PAP3 Pepper/Korea
RP4 Pepper/Korea
SP Spinach/Korea
PAP1 Pepper/Korea
RP6 Pepper/Korea
group A
LS2 Leonurus sibiricus/Korea
P2 Pea/Korea
P3 Pea/Korea
RP3 Pepper/Korea
BB5 Broad bean/Korea
XJ14-3 Tomato/China
Anhui Broad bean/China
Hunan Pepper/China
Ca Pepper/China
Am Atractylodes macrocephala/China
MB7 Broad bean/China
SN Gynura procumbens/Korea
PC Gentian/Korea
XJP1-1 Pepper/China
IA Gentian/Japan
Ty Gentian/Japan
SG1 Chinese yam/China
BRI Chinese yam/Korea
BR Chinese yam/Korea
DO Chinese yam/Korea
group B
LN Sesame/China
LNSY Chenopodium album/China
BBWV1-PV132
0.1
B
RNA2
GP4 Pepper/Korea
GP5 Pepper/Korea
GP2 Pepper/Korea
RP5 Pepper/Korea
RP1 Pepper/Korea
RP2 Pepper/Korea
SP1 Spinach/Korea
SP2 Spinach/Korea
BB9 Broad bean/Korea
RP6 Pepper/Korea
Anhui Broad bean/China
RP3 Pepper/Korea
RP4 Pepper/Korea
BB5 Broad bean/Korea
PAP3 Pepper/Korea
PAP2 Pepper/Korea
PAP1 Pepper/Korea
SP Spinach/Korea
P2 Pea/Korea
P3 Pea/Korea
group A
IA Gentian/Japan
MB7 Broad bean/China
SG1 Chinese yam/China
DO Chinese yam/Korea
BR Chinese yam/Korea
BRI Chinese yam/Korea
Hunan Pepper/China
SN Gynura procumbens/Korea
PC Gentian/Korea
Ty Gentian/Japan
XJ14-3 Tomato/China
XJP1-1 Pepper/China
Am Achyranthes bidentata/Korea
Ca Pepper/China
LNSY Chenopodium album/China
LN Sesame/China
LS2 Leonurus sibiricus/Korea
RP7 Pepper/Korea
BB2 Broad bean/Korea
IP Pepper/Japan
ME Megaskepasma erythrochlamys/Singapore
group B
AB1 Atractylodes macrocephala/China
BBWV1-PV132
0.1

**Figure. 2.** Phylogenetic analyses for the polyprotein amino acid sequences encoded by RNA1 (A) and RNA2 (B) of the broad bean wilt virus 2 (BBWV2) population. GenBank accession numbers of the analyzed BBWV2 isolates and strains are available in Table 1. Broad bean wilt virus 1 isolate PV132 (BBWV1-PV132) was included as an out-group. GenBank accession numbers of BBWV1-PV132: RNA1 (NC_005289) and RNA2 (NC_005290). Phylogenetic trees were reconstructed by the maximum-likelihood method applying the Jones-Taylor-Thornton model for amino acid sequence analyses. Numbers on the branches indicate bootstrap percentages based on 1,000 replications (only values >60% are shown). Collecting host and country of origin are indicated for each isolate (BBWV2 isolates collected from pepper are indicated with red letters). BBWV2 isolates PC, LS2, and P3 are indicated with blue arrowheads.

## 2. Genetic diversity of the BBWV2 population

To sought differences in divergence patterns, we performed genetic diversity analysis (Table 2). The amino acid diversities within and between groups in the phylogeny of each RNA segment. The analyses showed that the genetic diversity within group A in the RNA1 phylogeny was similar to that of group A in the RNA2 phylogeny (Table 2). On the other hand, the genetic diversity within group B in the RNA2 phylogeny was significantly higher than that of group B in the RNA1 phylogeny (Table 2). This result revealed that the isolates in group B in the RNA2 phylogeny have a higher degree of differentiation for RNA2 than RNA1.

**Table 2.** Amino acid diversity of the BBWV2 population

| Genome and subpopulation[a] | Amino acid diversity[b] within and between subpopulations | |
|---|---|---|
| **RNA1** | | |
| | group A | group B |
| group A | 0.022 ± 0.002 | |
| group B | 0.123 ± 0.008 | 0.039 ± 0.003 |
| **RNA2** | | |
| | group A | group B |
| group A | 0.020 ± 0.002 | |
| group B | 0.083 ± 0.006 | 0.089 ± 0.006 |

[a] Subpopulations were designated based on the phylogenetic trees shown in Figure. 1.
[b] Pairwise genetic diversity was analyzed by Poisson model using the MEGA X program. The numeric values indicate amino acid diversity ± standard error.

### 3. Evolutionary constraints on different genomic regions of the BBWV2 population

To examine whether different evolutionary constraints were applied on each BBWV2 gene, we analyzed pairwise genetic differences at nonsynonymous (*d*N) and synonymous (*d*S) nucleotide positions for each cistronic region. Comparison of diversity of the nucleotide sequences revealed that the genomic regions of the MP and LCP exhibited relatively low variability compared to those of the other genomic regions (Table 3). However, the *d*N/*d*S ratios of the MP- and LCP-coding regions were significantly higher than those of the other genomic regions except the Co-Pro-coding region (Table 3). The *d*N/*d*S ratio can reveal the type of selective constraints in molecular evolution (Kryazhimskiy and Plotkin 2008). In all, the results revealed that the MP- and LCP-coding regions in RNA2 and the Co-Pro-coding region in RNA1 have evolved under looser evolutionary constraints than the other genomic regions.

**Table 3.** Nucleotide diversity for different genomic regions of the BBWV2 population

| Genomic Region | | Nucleotide diversity[a] | | | |
|---|---|---|---|---|---|
| | | *d* | *d*N | *d*S | *d*N/*d*S |
| RNA1 | Co-Pro | 0.246 ± 0.025 | 0.132 ± 0.011 | 0.964 ± 0.108 | 0.137 |
| | NTBM | 0.121 ± 0.030 | 0.033 ± 0.004 | 1.214 ± 0.064 | 0.027 |
| | VPg | 0.159 ± 0.045 | 0.032 ± 0.019 | 0.994 ± 0.120 | 0.032 |
| | Pro | 0.170 ± 0.017 | 0.029 ± 0.006 | 1.054 ± 0.136 | 0.028 |
| | RdRp | 0.192 ± 0.033 | 0.030 ± 0.003 | 0.917 ± 0.222 | 0.033 |
| RNA2 | MP | 0.117 ± 0.036 | 0.057 ± 0.005 | 0.864 ± 0.064 | 0.066 |
| | LCP | 0.101 ± 0.034 | 0.065 ± 0.006 | 0.691 ± 0.052 | 0.094 |
| | SCP | 0.157 ± 0.011 | 0.026 ± 0.004 | 1.117 ± 0.096 | 0.024 |

[a] *d*, nucleotide diversity estimated by the Maximum Composite Likelihood method in MEGA X; *d*N and *d*S, nucleotide diversity at nonsynonymous and at synonymous position, respectively estimated by the Nei-Gojobori method in MEGA X; Values are means ± SEM.

**4. Pathogenic characterization of genetically distant BBWV2 isolates**

To examine whether the isolates phylogenetically distant or isolated from different hosts were also different in pathogenicity. To this end, we selected three isolates, PC, LS2, and P3, from our BBWV2 collection to investigate their pathogenicity in various plant species. The isolates, PC, LS2, and P3, have distant relationships in the phylogenetic trees, and were isolated from different host species, *G. scabra*, *L. sibiricus*, and *P. sativum*, respectively (Figure. 2). BBWV2 strain RP1 was included in the inoculation experiments as a reference strain since its pathogenicity was well characterized (Kwak et al. 2016). Identical results were obtained from at least three biological replicates in the inoculation experiments. The symptomatic responses to each isolate in the inoculated plant species are summarized in Table 3. In brief, the isolates LS2 and P3 had little symptomatic variations in the tested *Nicotiana* and *Capsicum* species. However, P3 caused necrotic symptoms in *C. amaranticolor*, *P. sativum*, and *V. faba*, while LS2 did not (Table 4). Meanwhile, the isolate PC showed obviously different pathogenicity from LS2 and P3 in the tested *Nicotiana* species: e.g., PC induced leaf malformation, yellowing, and stunting symptoms in *N. benthamiana*, while LS2 and P3 mainly caused mosaic symptom (Table 4). *S. oleracea* plants showed necrotic symptoms as well as leaf malformation and stunting when infected with P3, but showed mosaic symptoms when infected with LS2 and P3 (Table 4). Our results showed that the genetic diversification was accompanied by pathogenic differentiation in the BBWV2 population.

**Table 4.** Symptomatic variations of genetically distant BBWV2 isolates in various plant species

| Plant species | Symptomatic response to each BBWV2 isolates | | | |
|---|---|---|---|---|
| | **LS2** | **P3** | **PC** | **RP1** |
| *Nicotiana benthamiana* | M | M | LM,RS,St | MM |
| *N. occidentalis* | M | M | M, RS | MM |
| *Capsicum annuum L.* cv. Chungyang | M | M | MM | MM |
| *C. annuum L.* cv. Quari | M | M | MM | MM |
| *C. annuum L.* var. angulosum | M | M | MM | MM |
| *Cucumis sativus* cv. Dadagi | — | — | — | — |
| *Chenopodium amaranticolar* | LM,M | LM,NS | — | — |
| *C. quinoa* | LM,NS | LM,NS | LM,NS | LM,NS |
| *Perilla frutescens* | MM | MM | M,Y | MM |
| *Pisum sativum* | M | LM,NS | LM,M | M,St |
| *Solanum lycopersicum* cv. Ailsa Craig | — | — | — | — |
| *Spinacia oleracea* | MM | MM | LM,N,St | MM |
| *Vicia faba* | M | N,St | LM,St,Y | LM,Y |

[a]Symbols for symptoms: LM, leaf malformation; M, mosaic; MM, mild mosaic; N, necrosis; NS, necrotic spot; St, stunting; Y, yellowing; —, no infection.

**5. RNA2 determines the pathogenic characteristics of a BBWV2 isolate**

In our previous study, we showed that BBWV2 MP encoded in RNA2 functions as a determinant of symptom severity in pepper (Kwak et al. 2016; Seo et al. 2017). Moreover, our phylogenetic and diversity analyses revealed that BBWV2 RNA2 have higher genetic plasticity than RNA1 and may be associated with host adaptive evolution (Figure. 2 and Table 2, 3). Thus, we examined whether the pathogenic variation among the BBWV2 isolates is due to RNA2. The pathogenicity of pBBWV2-PC-R2 was examined by comparing with that of pBBWV2-RP1-R2 through pseudo-recombination with pBBWV2-RP1-R1. The pseudo-recombinant (pBBWV2-RP1-R1 + pBBWV2-PC-R2) induced the same symptoms of leaf malformation, yellowing, and stunting in *N. benthamiana* as the original isolate PC, whereas pBBWV2-RP1 (pBBWV2-RP1-R1 + pBBWV2-RP1-R2) induced mild mosaic symptoms (Figure. 3 and Table 4). The pathogenicity of the pseudo-recombinant was also the same as that of original isolate PC in *N. occidentalis*, some pepper cultivars, *P. frutescens*, *S. oleracea*, and *V. faba* (Figure. 3 and Table 4). Therefore, our results showed that the pathogenic characteristics of the isolate PC is determined by its RNA2.

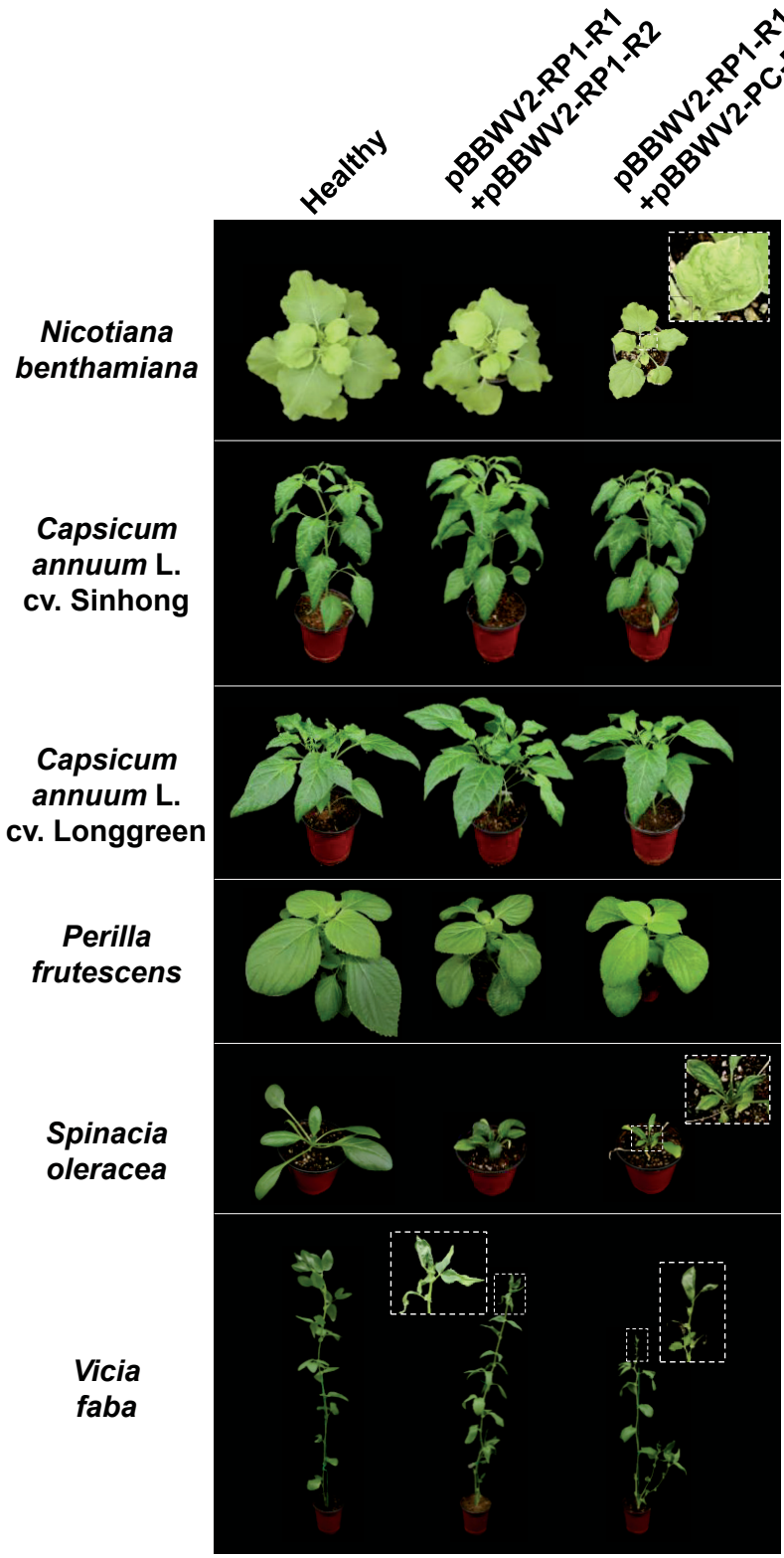
Healthy
pBBWV2-RP1-R1
+pBBWV2-RP1-R2
pBBWV2-RP1-R1
+pBBWV2-PC-R2
Nicotiana benthamiana
Capsicum annuum L. cv. Sinhong
Capsicum annuum L. cv. Longgreen
Perilla frutescens
Spinacia oleracea
Vicia faba

**Figure 3.** Virulence of the full-length cDNA clone of BBWV2-PC RNA2. Various plant plants were agroinoculated with infectious cDNA clones of pBBWV2-RP1-R1 and either pBBWV2-RP1-R2 or pBBWV2-PC-R2. Symptom development was monitored over 21 dpi. The pseudo-recombinant (pBBWV2-RP1-R1 + pBBWV2-PC-R2) induced the same symptoms as the original isolate PC in the tested plant species.

**6. Amino acid differences in RNA2 of BBWV2-RP1 and -PC**

RNA2 encodes a polyprotein precursor that is processed to yield three mature proteins, MP, LCP, and SCP. An amino acid sequence comparison between PC and RP1 in RNA2 showed that 42 amino acid differences are distributed through these three mature proteins (32, 5, and 5 amino acid differences in MP, LCP, and SCP, respectively) (Figure. 4). Specifically, a mutational hotspot was identified at the MP C-terminal region (Amino acid positions 424-442) (Figure. 4). Minimal differences in the amino acid sequence (even a single amino acid difference) of a viral protein can alter pathogenicity of the virus (Chen et al. 2008; Heo et al. 2020; Seo et al. 2011). Thus, further studies are in progress in our laboratory identify the viral protein(s) and amino acids responsible for the pathogenic characteristics of the isolate PC.

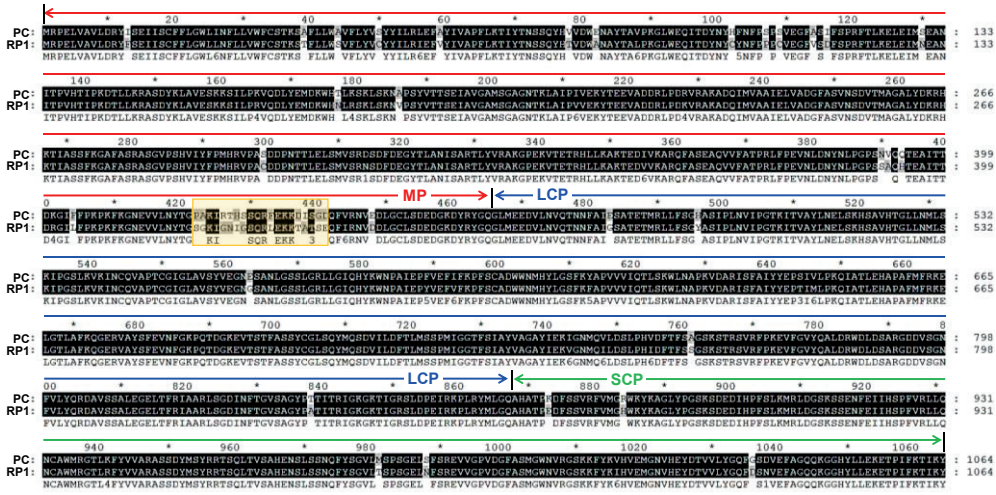


**Figure 4.** Amino acid differences between the polyproteins encoded in RNA2 of BBWV-PC and -RP1. The coding regions of the mature proteins, MP, LCP, and SCP, are indicated with red, blue, and green lines, respectively. A mutational hotspot at the MP C-terminal region is indicated with yellow box.

# DISCUSSION

Hosts act as important factors in the evolution of viruses because different hosts provide different selective environments to viruses (Garcia-Arenal et al. 2001; Heo et al. 2020; Safari and Roossinck 2018). Adaptation of a virus isolate to a particular host often involves genetic and pathogenic changes of the virus isolate to optimize its fitness in the particular host (Garcia-Arenal et al. 2001; Rico et al. 2006; Sacristan et al. 2005). Thus, adaptation to different hosts plays a critical role in the differentiation of a virus population. In this study, we examined whether genetic diversification is associated with pathogenic differentiation and host adaptation in the BBWV2 population. For this, three genetically distant BBWV2 isolates obtained from different hosts were compared for pathogenicity in various host species. Our inoculation experiments showed that there was significant pathogenic differentiation among the BBWV2 isolates from different hosts (Table 4).

The pathogenicity of a virus is a special evolutionary consequence of a trade-off between virus propagation and host adaptation (McLeish et al. 2018; Rico et al. 2006). Thus, the wide range of pathogenicity of a virus population may represent that it has a high evolutionary capacity. BBWV2 has a wide host range and causes diverse symptoms according to virus isolates and host plants, suggesting that it has a high divergence capacity for host adaptation. Indeed, our phylogenetic analyses of the BBWV2 population showed some genetic evidence for the host-adaptive evolution of BBWV2 (Figure. 2). In particular, most BBWV2 isolates from pepper were grouped together in the same clade. BBWV2 isolates from *Dioscorea opposita* also formed separated clades in both RNA1 and RNA2 phylogenies (Figure. 2). The degree of divergence among the isolates from the same hosts was significantly low, suggesting that

hosts may act as selective factors to restrict BBWV2 population diversity in each host (Figure. 2).

Our pathogenicity analysis with the infectious cDNA clones of BBWV2 RNA2 showed that a symptomatic determinant(s) of the isolate PC is located in its RNA2 (Figure. 3). A high genetic divergence level in RNA2 might be associated with symptomatic variation among the BBWV2 isolates (Table 2, 3). Viral proteins interact with various host proteins to form functional complexes, and sometimes their interactions with host resistance proteins trigger immune responses associated with symptoms, such as necrosis and chlorosis. In the meantime, mutational variations in the viral proteins can affect the intensity of the interactions with the host proteins. The changes in the intensity of these interactions may be directly related to the diversification of viral pathogenicity. Therefore, host-imposed constraints on RNA2 and its genetic plasticity have likely been contributed in genetic and pathogenic diversification of BBWV2 isolates and in shaping the structure of the BBWV2 population.

# REFERENCES

**Chen KC, Chiang CH, Raja JA, Liu FL, Tai CH, Yeh SD** (2008) A single amino acid of niapro of papaya ringspot virus determines host specificity for infection of papaya. Mol. Plant Microbe Interact. 21:1046-1057. doi:10.1094/MPMI-21-8-1046

**Choi B, Kwon SJ, Kim MH, Choe S, Kwak HR, Kim MK, Jung C, Seo JK** (2019) A Plant Virus-Based Vector System for Gene Function Studies in Pepper. Plant Physiol. 181:867-880. doi:10.1104/pp.19.00836

**de Wispelaere M, Rao ALN** (2009) Production of cucumber mosaic virus RNA5 and its role in recombination. Virology 384 (1):179-191. doi:https://doi.org/10.1016/j.virol.2008.10.023

**Ferrer RM, Ferriol I, Moreno P, Guerri J, Rubio L** (2011) Genetic variation and evolutionary analysis of broad bean wilt virus 2. Arch. Virol. 156:1445-1450. doi:10.1007/s00705-011-0990-3

**Garcia-Arenal F, Fraile A, Malpica JM** (2001) Variability and genetic structure of plant virus populations. Annu. Rev. Phytopathol. 39:157-186. doi:10.1146/annurev.phyto.39.1.157

**Heo KJ, Kwon SJ, Kim MK, Kwak HR, Han SJ, Kwon MJ, Rao ALN, Seo JK** (2020) Newly emerged resistance-breaking variants of cucumber mosaic virus represent ongoing host-interactive evolution of an RNA virus. Virus Evol. 6:veaa070. doi:10.1093/ve/veaa070

**Kryazhimskiy S, Plotkin JB** (2008) The population genetics of dN/dS. PLoS Genet. 4:e1000304. doi:10.1371/journal.pgen.1000304

**Kumar S, Stecher G, Li M, Knyaz C, Tamura K** (2018) MEGA X: Molecular Evolutionary Genetics Analysis across Computing Platforms. Molecular Biology and Evolution 35 (6):1547-1549. doi:10.1093/molbev/msy096

**Kwak HR, Kim MK, Lee YJ, Seo JK, Kim JS, Kim KH, Cha B, Choi HS** (2013a) Molecular Characterization and Variation of the Broad bean wilt virus 2 Isolates Based on Analyses of Complete Genome Sequences. Plant Pathol. J. 29:397-409. doi:10.5423/PPJ.OA.03.2013.0036

**Kwak HR, Kim MK, Nam M, Kim JS, Kim KH, Cha B, Choi HS** (2013b) Genetic Compositions of Broad bean wilt virus 2 Infecting Red Pepper in Korea. Plant Pathol. J. 29:274-284. doi:10.5423/PPJ.OA.12.2012.0190

**Kwak HR, Lee YJ, Kim J, Kim MK, Kim JS, Choi HS, Seo JK** (2016) A determinant of disease symptom severity is located in RNA2 of broad bean wilt virus 2. Virus Res. 211:25-28. doi:10.1016/j.virusres.2015.09.018

**McLeish MJ, Fraile A, Garcia-Arenal F** (2018) Ecological Complexity in Plant Virus Host Range Evolution. Adv Virus Res 101:293-339. doi:10.1016/bs.aivir.2018.02.009

**Rico P, Ivars P, Elena SF, Hernandez C** (2006) Insights into the selective pressures restricting Pelargonium flower break virus genome variability: Evidence for host adaptation. J. Virol. 80:8124-8132. doi:10.1128/JVI.00603-06

**Sacristan S, Fraile A, Malpica JM, Garcia-Arenal F** (2005) An Analysis of Host Adaptation and Its Relationship with Virulence in Cucumber mosaic virus. Phytopathology 95:827-833. doi:10.1094/PHYTO-95-0827

**Safari M, Roossinck MJ** (2018) Coevolution of a Persistent Plant Virus and Its Pepper Hosts. Mol. Plant Microbe Interact. 31:766-776. doi:10.1094/MPMI-12-17-0312-R

**Seo JK, Kwak HR, Choi B, Han SJ, Kim MK, Choi HS** (2017) Movement protein of broad bean wilt virus 2 serves as a determinant of symptom severity in pepper. Virus Res. 242:141-145. doi:10.1016/j.virusres.2017.09.024

**Seo JK, Lee SH, Kim KH** (2009) Strain-specific cylindrical inclusion protein of soybean mosaic virus elicits extreme resistance and a lethal systemic hypersensitive response in two resistant soybean cultivars. Mol. Plant Microbe Interact. 22:1151-1159. doi:10.1094/MPMI-22-9-1151

**Seo JK, Shin OJ, Kwak HR, Kim MK, Choi HS, Lee SH, Kim JS** (2014) First Report of Broad bean wilt virus 2 in Leonurus sibiricus in Korea. Plant Dis. 98:1748. doi:10.1094/PDIS-07-14-0695-PDN

**Seo JK, Sohn SH, Kim KH** (2011) A single amino acid change in HC-Pro of soybean mosaic virus alters symptom expression in a soybean cultivar carrying Rsv1 and Rsv3. Arch. Virol. 156:135-141. doi:10.1007/s00705-010-0829-3

# Chapter 2

# Molecular characterization of the interactions between broad bean wilt virus 2 VP37 and heat shock protein 90

# INTRODUCTION

Plants as sessile organisms are continuously exposed to a variety of abiotic or biotic stresses that can either directly limit their growth or cause metabolic dysfunction (Atkinson and Urwin 2012; Rejeb et al. 2014; Suzuki et al. 2014; Syller and Grupa 2016; Tanaka et al. 2014). Plant viruses are one of the biotic stresses that can infect plants and are obligate parasites that lead their life cycle by hijacking the metabolic functions and cellular machinery of plants (Osterbaan and Fuchs 2019). The infectious process of these viruses is a complex procedure involving the interaction between viruses and various host factors (Liu and Nelson 2013). Through the interaction between the virus component and the host factor, viruses can penetration into the host, replication, recombination, and movement within the host. In this process, the virus affects the various gene regulate systems of the host, and is accompanied by rapid physiological changes within the host. These changes are not always the case but are often manifested macroscopically as a symptom of the disease (Carbonell et al. 2016; Pallas and Garcia 2011).

Plant viruses spread from cell to cell pass through via plasmodesmata (PD) for systemic infection. This is because the plant viruses do not utilize membrane fusion and cannot degrade the cell wall (Genovés et al. 2009; Navarro et al. 2019). Thus, viruses use host factors to move from the viral replication site to the plasma membrane and the cell wall within the cell and to move from the cell wall to other adjacent cells by modifying the size exclusion limit (SEL) of the PD (Navarro et al. 2019). To perform these functions, the viruses encode one or more non-structural factors known as transfer protein(s). One of the components of the virus, the movement protein (MP), is responsible for enabling the virus to move from cell to cell and throughout the whole plant (Navarro et al. 2019; Seo and Kim 2016). Although numerous identified MPs

so far have structural differences between each other, most MPs share similar properties such as RNA binding ability, interaction with viral and host factors, and the gating ability of PD. It is involved in the transport of infectious substances, either virion or viral ribonuclear proteins (vRNP) (Genovés et al. 2009; Lucas 2006; Waigmann et al. 2004). And many MPs are associated with the endoplasmic reticulum (ER) and cytoskeletal elements and are identified as cell membrane proteins that rely heavily on cellular macromolecular transport systems for viral transport (Genovés et al. 2009; Nelson and Citovsky 2005). MP transfers viruses using two mechanisms. The one is a non-tubule-guided movement, where MP interacts with viral RNA and the host factor, the ER, to form a vRNP, allowing transport of vRNP through PD without causing visual changes. The second is a tubule-guided movement, which expands the PD by forming a desmotubule composed of MP complex inside the PD, and moves the virion through the passage (Kasteel et al. 1996; Niehl and Heinlein 2011; Ritzenthaler and Hofmann 2007; Wellink et al. 1993). It is well known that several viral MPs are involved in the viral movement by interacting with host factors of various plant species (Chen et al. 2000; Kaido et al. 2007; Link and Sonnewald 2016; Uhrig and MacFarlane 2008).

Broad bean wilt virus2 (BBWV2), one of the genus *Fabavirus* in the family *Secoviridae*, It has a wide host range and infects various agricultural products and horticultural crops around the world (Ferrer et al. 2011; Kwak et al. 2013). BBWV2 is easily transmitted in a non-persistent manner by aphids, mostly *Aphis gossypii* and *Myzus persicae*. The BBWV2 genome is composed of two segmented positive stranded RNAs, RNA1 (≅5.8 kb) and RNA2 (≅3.3 kb), which are encapsidated separately into icosahedral virions (Atsumi et al. 2013; Ferrer et al. 2011). The 5’ end of each is linked to viral genome-linked protein (VPg), and the 3’ end is polyadenylated. Each RNA segment contains a single open reading frame (ORF) that translated into one large single polyprotein precursor. The polyprotein precursor encoded by BBWV2 RNA1 is processed

by proteolytic cleavage to yield five mature proteins: protease cofactor (Co-Pro), Helicase (Hel), VPg, protease (Pro), and RNA-dependent RNA polymerase (RdRp). Also the polyprotein precursor encoded by RNA2 is processed to yield four mature proteins: 53kDa / 37kDa proteins (VP53 / VP37; MP), large coat protein (LCP), and small coat protein (SCP) (Ferrer et al. 2011; Kwak et al. 2013). Therefore, RNA1 plays a role in viral proliferation, and RNA2 is involved in viral cell-to-cell movement and encapsidation (Liu et al. 2011; Xie et al. 2016). The 53kDa protein of BBWV2 RNA2 can be divided into 53kDa / 37kDa (VP53 / VP37) proteins. These proteins have an overlapping region at the C-terminus and have two translation initiation sites by the virus's replication strategy, leaky ribosomal scanning (Kong et al. 2014). The VP37 protein is a multifunctional protein that binds to single-stranded nucleic acids, interacts with the viral CP, and potentiates viral intercellular transport within the host plant. However, the features of the VP53 are not yet clear (Kong et al. 2014; Liu et al. 2009; Liu et al. 2011). And BBWV2 VP37 has been reported to move using tubule-guided movement, but there is no known which host factors interact with BBWV2-MP to enable the movement of virus in this process, so more research is needed (Liu et al. 2011; Xie et al. 2016).

In this study, we tried to identify host genes that are highly related to BBWV2-MP to understand the molecular interactions between viruses and host proteins. Using a proteomic approach, host factors that interact with BBWV2-MP have been identified by co-immunoprecipitation (co-IP) in the model plant *Nicotiana benthamiana*. The identified candidate host genes interacted directly with BBWV2-MP through yeast two-hybrid (Y2H) to further verify whether they are involved in virus movement. We tried to find out the fundamental knowledge about BBWV2 through this study.

# MATERIALS AND METHODS

## 1. Plant growth condition

*N. benthamiana* was grown in a growth chamber under 16 h/24°C day and 8 h/20°C night conditions. After agroinfiltration with pBBWV2 infectious clones, plants were grown in the same condition.

## 2. Agrobacterium-mediated inoculation

Plasmid DNAs for Agro-transformation were prepared using the Plasmid Miniprep Kit (QIAGEN, USA). *Agrobacterium tumefaciens* strain EHA105 was transformed with approximately 2 μg of plasmid DNA by freeze-thaw method. For subcellular localization, pBBWV2-PAP1-R1, pBBWV2-R2-GFP, were inoculated to 5 ml LB broth with kanamycin (100 μg/μl) and rifampicin (50 μg/μl) and incubated in shaking incubator at 220 rpm at 28°C for 9 h. The culture was resuspended to $OD_{600}$ of 0.5 with infiltration buffer (10 mM MES, 10 mM $MgCl_2$, and 200 μM acetosyringone, pH 5.6). Resuspended cultures were incubated in 28°C shaking incubator at 220 rpm for 4 h. pBBWV2 RNA1 and RNA2 were mixed together in equal proportions and infiltrated onto the abaxial surface of 2 weeks old *N. benthamiana* leaves using 1 ml needleless syringe and the PD marker aniline blue also infiltrated onto the *N. benthamiana* as a control. For co-IP, pBBWV2-PAP1-R1, pBBWV2-PAP1-R2-MP-B2 and pBBWV2-R2-MP:F-B2 were inoculated to 5 ml LB broth with kanamycin (100 μg/μl) and rifampicin (50 μg/μl) and incubated in shaking incubator at 220 rpm at 28°C for 9 h. The cultures were resuspended to $OD_{600}$ of 0.5 with infiltration buffer (10 mM MES, 10 mM $MgCl_2$, and 200 μM acetosyringone, pH 5.6). Resuspended cultures were incubated in 28°C shaking incubator at 220 rpm for 4 h. pBBWV2 RNA2 cultures were mixed together with pBBWV2 RNA1 in equal proportions and infiltrated onto the abaxial surface of 2 weeks

old *N. benthamiana* leaves using 1 ml needleless syringe.

### 3. Confocal microscopic analysis

The agroinfiltrated *N. benthamiana* leaves at 7 days post infiltration (dpi) for subcellular localization were cut into 5 x 5 $mm^2$ pieces were placed on a slide glass with water and used for confocal microscopic analysis. The fluorescence was imaged using a Leica TCS SP8 STED (Leica, Wetzlar, Germany) equipped with a specific laser/filter combination to detect GFP (excitation at 488 nm), CFP (excitation at 458 nm). LAS X software (Leica) was used to analyze the images.

### 4. Tagging BBWV2 genes by engineering infectious cDNA clones

Recognition sites of restriction enzymes (NEB, USA) were used in the pBBWV2-PAP1-R2 clone, and FLAG-tag was fused to the C-terminal of BBWV2-MP for co-IP. FLAG sequence was added to MP by PCR with 2 primers for pBBWV2-R2-MP:F-B2 (Fw: 5'- GCTTCAGTCAATTCGGATG TTAC - 3' and Rv: 5'- ATCGCCTAGGCTTGTCATCGTCGTCCTTGTAGT CTTGACCATATCTATAATCTTTGCC -3'). The reverse primer contains the Flag sequence. Using *Nco*I, *Avr*II restriction enzyme digestion and ligated to make pBBWV2-PAP1-R2-MP-B2 and MP:F.

### 5. SDS-PAGE and Western blot

Western blot was conducted to confirm whether MP:Flag proteins were expressed in *N.benthamana*. Total protein extraction from *N.benthamana* leaves was performed using the TRIzol™ Reagent methods (Invitrogen, USA) according to the manufacturer's instructions. Total proteins for each sample were separated by 12% SDS-PAGE and transferred onto the PVDF membrane. Proteins were probe with an anti-FLAG antibody (1:1000) (Clontech, Japan), and an anti-mouse antibody (1:5000) was used as the secondary antibody.

Immunoreactions were detected using the ECL-based system (Sigma-Aldrich, USA).

## 6. Co-immunoprecipitation and LC-MS/MS analysis

Total protein extracts were prepared from the infected leaves of *N. benthamiana* plants inoculated with pBBWV2-PAP1-R1/pBBWV2-PAP1-R2-MP-B2 and pBBWV2-PAP1-R1/pBBWV2-PAP1-R2-MP:F-B2. At 7 dpi, the leaves were homogenized in liquid nitrogen and add 2.5 ml of protein extraction buffer (1M Tris–HCl at pH 7.5, 5M NaCl, 1M $MgCl_2$, 1M DTT, 1% CHAPS, proteinase inhibitor cocktail (Sigma, USA). Cell debris was removed by centrifugation at 13,500 rpm for 10 min at 4°C using cell strainers. The resulting supernatants were incubated with anti-FLAG antibody conjugated magnetic beads (ThermoFisher, USA) for overnight at 4°C. The immunocomplexes were then precipitated by centrifugation for 10 min at 12,000 rpm and washed five times in 1 mL of the protein extraction buffer. The resulting samples were analyzed by 12% SDS-PAGE and stained with coomassie blue. Used the Xpert prestained protein marker (GenDEPOT, USA) as the ladder. After staining, bands of interest were excised from the gel and analyzed by liquid chromatography-tandem mass spectrometry (LC-MS/MS). The LC-MS/MS analysis was performed at Yonsei Proteome Research Center (Seoul, South Korea). To identify and quantify peptides, LC was performed with an Easy n-LC 1000 system (Thermo Fisher Scientific, Rockford, IL, USA). A C18-nanobore column (150 mm × 0.1 mm, 3-μm pore size, Agilent) was used for peptide separation. LTQ-Orbitrap mass spectrometry (Thermo Fisher, USA) was used to identify and quantify peptides. Xcalibur (version 2.1, Thermo Fisher Scientific, USA) was used to generate peak lists. The peak lists were examined by searching the National Center for Biotechnology Information (NCBI) database using the MASCOT search engine (http://www.matrixscience.com, Matrix Science, Boston, MA, USA). The

acquired data were compared to the whole database with search parameters set as follows: enzyme, trypsin; allowance of up to one missed cleavage peptide; mass tolerance ± 0.5 Da and MS/MS tolerance ± 0.5 Da; modifications of methionine oxidation and cysteine carbamidomethylation when appropriate, with auto hits allowed and only significant hits to be reported. The proteins were identified on the basis of two or more peptides whose ion scores exceeded the threshold, $P < 0.05$, which indicated the 95% confidence level for these matched peptides.

## 7. Clone construction for yeast two-hybrid assay

### 7. 1. Cloning of intact and truncated genes

In host factors, total RNA was extracted using the Hybrid-R$^{TM}$ (GeneAll, Korea) from *N. bentamiana* and cDNA was synthesized using specific primers for each gene (Table 1). Total RNA was denatured at 65°C for 5 min with 10 μM of the reverse primer. The RT reaction was incubated at 50°C for 30 min with SuperScript IV Reverse Transcriptase (Invitrogen, USA). cDNA was amplified using Q5 High-Fidelity DNA polymerase (NEB, USA) appropriate primer pairs for the full length of host genes (Table 2). In BBWV2 (VP37, VP53), PCR was performed using pBBWV2-PAP1-MP-B2 plasmid with suitable primer pairs (Table 3). In NbHsp90-2, the truncated clones were amplified using appropriate primer pairs and full length of NbHsp90-2 plasmid (Table 4). In VP37, the truncated VP37 were amplified using appropriate primer pairs and the full length of the VP37 plasmid (Table 5).

### 7. 2. Cloning of amino acid substitution mutants

In NbHsp90-2, the single conversion of the negatively charged amino acids glutamate (Glu) such as E3, E5, and E12 into uncharged amino acid alanine (Ala) and the single conversion of the glutamate into same negatively charged amino acid Aspartate (Asp), both nonpolar and negatively charged amino acid

change were conducted using pGADT7-NbHsp90-2 for the template. NbHsp90-$2^{E3A}$ and NbHsp90-$2^{E5A}$ substitution using appropriate primer pairs for PCR (NbHsp90-$2^{E3A}$-Fw/NbHsp90-2-Rv2, NbHsp90-$2^{E5A}$-Fw/NbHsp90-2-Rv2). E12A substitution using appropriate primer pairs (NbHsp90-$2^{E12A}$-Fw/NbHsp90-$2^{E12A}$-Rv) for PCR by Q5® Site-Directed Mutagenesis Kit (NEB, USA). The double amino acid conversion of the $E^5$, $E^{12}$ amino acid to Ala or Asp using pGADT7-NbHsp90-$2^{E12A}$ or -NbHsp90-$2^{E12D}$ for template and appropriate primer pairs (NbHsp90-$2^{E12A}$, NbHsp90-$2^{E12D}$) for PCR by Q5® Site-Directed Mutagenesis Kit (NEB, USA) (Table 6).

In VP37, the single amino acid conversion of the positive charged amino acids, Lysine (Lys) and Arginine (Arg), such as $K^{31}$, $K^{32}$, and $R^{37}$ into uncharged amino acid Ala. In the truncated VP37, single amino acid substitution using pGBKT7-$VP37^{31\text{-}337}$ for template and appropriate primer pairs ($VP37^{31\text{-}337\text{-}31A}$, $VP37^{31\text{-}337\text{-}32A}$, $VP37^{31\text{-}337\text{-}37A}$) for PCR. In the full length of VP37, Single or double amino acid substitution using pGBKT7-VP37 for template and appropriate primer pairs ($VP37^{31A}$, $VP37^{32A}$, $VP37^{37A}$, $VP37^{40,43A}$) for PCR by Q5® Site-Directed Mutagenesis Kit (NEB, USA). Triple amino acid substitution using pGBKT7-$VP37^{37A}$ plasmid for template and $VP37^{31,32A}$ primer pair for PCR. The triple amino acid substitution of the $K^{31}$, $K^{32}$, and $R^{37}$ into Ala using pGBKT7-$VP37^{37A}$ for template and $VP37^{31,32A}$ primer pair. The double amino acid substitution of the negatively charged amino acid $D^{40}$, $E^{43}$ into alanine using pGBKT7-VP37 for template and $VP37^{40,43A}$ primer pair (Table 7).

The pGBKT7 vector harboring the GAL4 DNA binding domain (BD) and the pGADT7 vector harboring the GAL4 DNA activation domain (AD). Both vectors were used for the Yeast two-hybrid (Y2H) screen (Takara. US) and were enzyme digested with restriction enzymes (NEB. USA) suitable for each gene. For VP37 and VP53, the vectors and inserts were digested by the restriction enzyme *Eco*RI, *Bam*HI. For NbHsp90s, the vectors were digested

by the restriction enzyme *Sma*I and *Xho*I, and the inserts were digested by the restriction enzyme only *Xho*I, the *Sma*I sticky end site added the sequence by PCR. NbHsp90-3 was obtained during the screening process of NbHsp90-2. For pGADT7-NbHOP3, the vectors and inserts were enzyme digested by the restriction enzyme *EcoR*I, *Xho*I. For NbHsp70, the pGADT7 and insert digested by the restriction enzyme *Nde*I, *BamH*I. After digested all fragments cloned into each vector using T4 DNA ligase (NEB, USA).

**8. Yeast Two-Hybrid assay**

The pGBKT7 and the pGADT7 vectors were co-transformed into the yeast strain AH109 (Clontech, USA) using the LiAC/SS carrier DNA/PEG method (Gietz and Woods 2002). An X-α-Gal assay using the X-α-Gal protocol-at-a-Glance (Clontech, USA). The transformants were mixed with 150 µl of distilled water ($ddH_2O$) then dropped onto double-out (SD/-Leu/-Trp) and triple-out (SD/-Leu/-Trp/-His) selection medium plate by 40 µl at 28°C. The positively grown yeasts were picked on the double plate and re-cultivated in the double-out or triple-out liquid medium. After the $OD_{600}$ values were adjusted to 0.3 and 0.03 using ddH2O, it was dropped out on double-out, triple-out, triple-out containing X-α-Gal, and quadruple-out (SD/Leu/-Trp/-His/-Ade) selection medium plate at 28°C.

**Table 1.** List of primers for reverse transcription primer of host factors

| Gene | Primer name | Sequence (5' to 3') |
|---|---|---|
| NbBLP4 | NbBLP4-BamHI-Rv2 | CGGGATCCTACAGCTCGTCATGATCRTCATC |
| NbHOP3 | NbHOP3-RT | CTGGAAAGCCAGAGAAAGAAC |
| NbHsp90s | NbHsp90-2-RT | GAGTTARTCAACTTCCTCCATCT |
| NbHsp70 | Hsp70-RT | CGATCACGCTATCTTAAAGCC |

R: A+G



**Table 2.** List of primers for PCR of full length of host factors

| Gene | Primer name | Sequence (5' to 3') | Position | Length | Accession No. |
|---|---|---|---|---|---|
| NbHsp90-1 | NbHsp90-1-SmaI-1-Fw | GATGGCGGACACAGAAACCTTTGCTTTT | 1-2100 | 2100 | KT726858.1 |
| | NbHsp90-1-XhoI-2100-Rv | ACTCGCTCGAGTTAATCGACTTCTTCCATCTTGCTGCCT | | | |
| NbHsp90-2 | NbHsp90-2-Fw2 | GATGGCGGAGGMRGAGACGTT | 1-2100 | 2100 | KT726859.1 |
| | NbHsp90-2-Rv2 | ACTCGCTCGAGTTARTCAACTTCCTCCATCTTGCT | | | |
| NbHOP3 | NbHOP3-EcoRI-Fw | CGGAATTCATGGCCGACGAAGCGAAGGCGAAA | 1-1770 | 1770 | |
| | NbHOP3-XhoI-1770-Rv | ACTCGCTCGAGTTATTTGACTTGAATAATTCCTGCAC | | | |
| NbHsp70 | Hsp70-NdeI-Fw | GGAATTCCATATGATGGCAGGAAAAGGTGAAGG | 1-1950 | 1950 | |
| | Hsp70-BamH1-Rv | CGGGATCCTTAGTCGACCTCCTCAATC | | | |

R: A+G, M: A+C

**Table 3.** List of primers for PCR of BBWV2 movement protein

| Gene | Primer name | Sequence (5' to 3') | Position | Length |
|---|---|---|---|---|
| VP53 | BBWV2-PAP1mp-EcoRI-Fw | ACGAATTCATGCGTCCCGAACTTGTTG | 1-1395 | 1395 |
| | BBWV2-PAP1mp-BamHI-Stop-Rv | CGGGATCCTATTGACCATATCTATAATC | | |
| VP37 | BBWV2-PAP1mp37-EcoRI-Fw | ACGAATTCATGAATGAGGCAAATATCAC | 385-1395 | 1011 |
| | BBWV2-PAP1mp-BamHI-Stop-Rv | CGGGATCCTATTGACCATATCTATAATC | | |

R: A+G, M: A+C

**Table 4.** List of primers for PCR of truncated NbHsp90-2

| Name | Primer pairs | Sequence (5' to 3') | Position | Length |
|---|---|---|---|---|
| ΔhC:NbHsp90-2 | NbHsp90-2-Fw2 | GATGGCGGAGGMRGAGACGTT | 1-1800 | 1800 |
| | NbHsp90-2-XhoI-1800-Rv | ACTCGCTCGAGAGACATGTATCCAGCCATGC | | |
| ΔhN:NbHsp90-2 | NbHsp90-2-Sma1-301-Fw | GGGGACCAAGGAATTTATGGAG | 301-2100 | 1800 |
| | NbHsp90-2-Rv2 | ACTCGCTCGAGTTARTCAACTTCCTCCATCTTGCT | | |
| NbHsp90-2-51-700 | NbHsp90-2-Sma1-151-Fw | GTTGACTGACAAGAGCAAGCT | 151-2100 | 1950 |
| | NbHsp90-2-Rv2 | ACTCGCTCGAGTTARTCAACTTCCTCCATCTTGCT | | |
| NbHsp90-2-26-700 | NbHsp90-2-Sma1-76-Fw | GAGCAACAAAGAGATCTTTCTC | 76-2100 | 2025 |
| | NbHsp90-2-Rv2 | ACTCGCTCGAGTTARTCAACTTCCTCCATCTTGCT | | |
| ΔhNC:NbHsp90-2 | NbHsp90-2-Sma1-301-Fw | GGGGACCAAGGAATTTATGGAG | 301-1800 | 1500 |
| | NbHsp90-2-XhoI-1800-Rv | ACTCGCTCGAGAGACATGTATCCAGCCATGC | | |

R: A+G, M: A+C

**Table 5.** List of primers for PCR of truncated VP37

| Name | Primer pairs | Sequence (5' to 3') | Position | Length |
|---|---|---|---|---|
| Δ1/3C:VP37 | BBWV2-PAP1mp37-EcoRI-Fw | ACGAATTCATGAATGAGGCAAATATCAC | 1-675 | 675 |
| | VP37-BamHI-675-Rv | CGGGATCCCTCAGTCTTGGCTTTCAAAAG | | |
| Δ1/6C:VP37 | BBWV2-PAP1mp37-EcoRI-Fw | ACGAATTCATGAATGAGGCAAATATCAC | 1-843 | 843 |
| | VP37-BamHI-843-Rv | CGGGATCCTTTTGGCTTTGGAAACAATATTC | | |
| VP37-1-308 | BBWV2-PAP1mp37-EcoRI-Fw | ACGAATTCATGAATGAGGCAAATATCAC | 1-924 | 924 |
| | VP37-BamHI-924-Rv | CGGGATCCTTTCTTCTCAAATCTCTGAGG | | |
| VP37-1-326 | BBWV2-PAP1mp37-EcoRI-Fw | ACGAATTCATGAATGAGGCAAATATCAC | 1-978 | 978 |
| | VP37-BamHI-978-Rv | CGGGATCCAGACAGGCATCCAAGATCATC | | |
| Δ1/3N:VP37 | VP37-EcoRI-337-Fw | GGAATTCAAGAAATCCATCTTGCCAAGA | 337-1011 | 675 |
| | BBWV2-PAP1mp-BamHI-Stop-Rv | CGGGATCCTATTGACCATATCTATAATC | | |
| Δ1/6N:VP37 | VP37-EcoRI-169-Fw | GGAATTCAACGTTCCTAGCTACGTCAC | 169-1011 | 843 |
| | BBWV2-PAP1mp-BamHI-Stop-Rv | CGGGATCCTATTGACCATATCTATAATC | | |
| VP37-31-337 | VP37-EcoRI-91-Fw | GGAATTCATGGACAAGTGGCACAACTTG | 91-1011 | 921 |
| | BBWV2-PAP1mp-BamHI-Stop-Rv | CGGGATCCTATTGACCATATCTATAATC | | |
| VP37-44-337 | VP37-EcoRI-130-Fw | GGAATTCACATTGCTTAAGAGAGCGAG | 130-1011 | 882 |
| | BBWV2-PAP1mp-BamHI-Stop-Rv | CGGGATCCTATTGACCATATCTATAATC | | |
| VP37-16-337 | VP37-EcoRI-46-Fw | GGAATTCATTGAGTTGGTGGCGGATGG | 46-1011 | 966 |
| | BBWV2-PAP1mp-BamHI-Stop-Rv | CGGGATCCTATTGACCATATCTATAATC | | |
| VP37-113-225 | VP37-EcoRI-337-Fw | GGAATTCAAGAAATCCATCTTGCCAAGA | 337-675 | 339 |
| | VP37-BamHI-675-Rv | CGGGATCCCTCAGTCTTGGCTTTCAAAAG | | |

**Table 6.** List of primers for PCR of amino acid substitution of NbHsp90-2

| Name | Primer pairs | Sequence (5' to 3') | Position | Length |
|---|---|---|---|---|
| NbHsp90-2-E3A | NbHsp90-2-E3A-Fw | GATGGCGGCGGCGGAGACGTT | 1-2100 | 2100 |
| | NbHsp90-2-Rv2 | ACTCGCTCGAGTTARTCAACTTCCTCCATCTTGCT | | |
| NbHsp90-2-E5A | NbHsp90-2-E5A-Fw | GATGGCGGAGGCGGCGACGTT | 1-2100 | 2100 |
| | NbHsp90-2-Rv2 | ACTCGCTCGAGTTARTCAACTTCCTCCATCTTGCT | | |
| NbHsp90-2-E12A | NbHsp90-2-E12A-Fw | TTTCCAAGCTGCGATCAACCAGCTG | 1-10059 | 10059 |
| | NbHsp90-2-E12A-Rv | GCAAACGTCTCCGCCTCC | | |
| NbHsp90-2-E3D | NbHsp90-2-E3D-Fw | GATGGCGGACGCGGAGACGTT | 1-2100 | 2100 |
| | NbHsp90-2-Rv2 | ACTCGCTCGAGTTARTCAACTTCCTCCATCTTGCT | | |
| NbHsp90-2-E5D | Hsp90-2-E5D-Fw | GATGGCGGAGGCGGACACGTT | 1-2100 | 2100 |
| | NbHsp90-2-Rv2 | ACTCGCTCGAGTTARTCAACTTCCTCCATCTTGCT | | |
| NbHsp90-2-E12D | NbHsp90-2-E12D-Fw | TTTCCAAGCTGACATCAACCAGCTGTTG | 1-10059 | 10059 |
| | NbHsp90-2-E12D-Rv | GCAAACGTCTCCGCCTCC | | |

**Table 7.** List of primers for PCR of amino acid substitution of VP37

| Name | Primer pairs | Sequence (5' to 3') | Position | Length |
|---|---|---|---|---|
| VP37-31-337-E31A | VP37-EcoRI-E31A-Fw | GGAATTCGCGAAATCCATCTTGCCAAGA | 130-1011 | 882 |
| | BBWV2-PAP1mp-BamHI-Stop-Rv | CGGGATCCTATTGACCATATCTATAATC | | |
| VP37-31-337-E32A | VP37-EcoRI-E32A-Fw | GGAATTCAAGGCGTCCATCTTGCCAAGA | 130-1011 | 882 |
| | BBWV2-PAP1mp-BamHI-Stop-Rv | CGGGATCCTATTGACCATATCTATAATC | | |
| VP37-31-337-E37A | VP37-EcoRI-E37A-Fw | GGAATTCAAGAAATCCATCTTGCCAGCGGTGCAA | 130-1011 | 882 |
| | BBWV2-PAP1mp-BamHI-Stop-Rv | CGGGATCCTATTGACCATATCTATAATC | | |
| VP37-31A | VP37-E31A-Fw | TGTGGAGAGCGCGAAATCCATCTTG | 1-8310 | 8310 |
| | VP37-E31A-Rv | GCTAATTTGTAGTCACTCG | | |
| VP37-32A | VP37-E32A-Fw | GGAGAGCAAGGCGTCCATCTTGCC | 1-8310 | 8310 |
| | VP37-E32A-Rv | ACAGCTAATTTGTAGTCAC | | |
| VP37-37A | VP37-E37A-Fw | CATCTTGCCAGCGGTGCAAGATTTGTATG | 1-8310 | 8310 |
| | VP37-E37A-Rv | GATTTCTTGCTCTCCACAG | | |
| VP37-31,32A | VP37-E31,32A-Fw | TGTGGAGAGCGCGGCGTCCATCTTGCCAGC | 1-8310 | 8310 |
| | VP37-E31,32A-Rv | GCTAATTTGTAGTCACTCG | | |
| VP37-40,43A | VP37-D40A,E43A-Fw | TATGCGATGGACAAGTGGCACAAC | 1-8310 | 8310 |
| | VP37-D40A,E43A-Rv | CAACGCTTGCACTCTTGGCAAGATG | | |

# RESULT

## 1. Subcellular localization of BBWV2-MP

In order to observe where the viral MP is localized by interacting with the host factor through an in vivo experiment, pBBWV2-R2-GFP, which can overexpress GFP reported in our previous paper, was used (Figure 1A) (Choi et al. 2019). The regulation of localization may differ from virus to virus, as it is determined by the presence of other viral components or by changes in the cellular environment induced by the virus (Wang et al. 2017). It has been reported that BBWV2 forms a tubule during movement and expands the size of PD (Xie et al. 2016), and our clone was able to sufficiently express GFP during replication, which was encapsulated with the proteins of BBWV2 to prevent viral movement. This suggests that our data are sufficiently visibly verifiable. The data showed that BBWV2-MP spread along the membrane through co-localization of GFP. Among them, it was found that the dot expressing strong GFP was co-localized with the PD marker (Figure 1B).

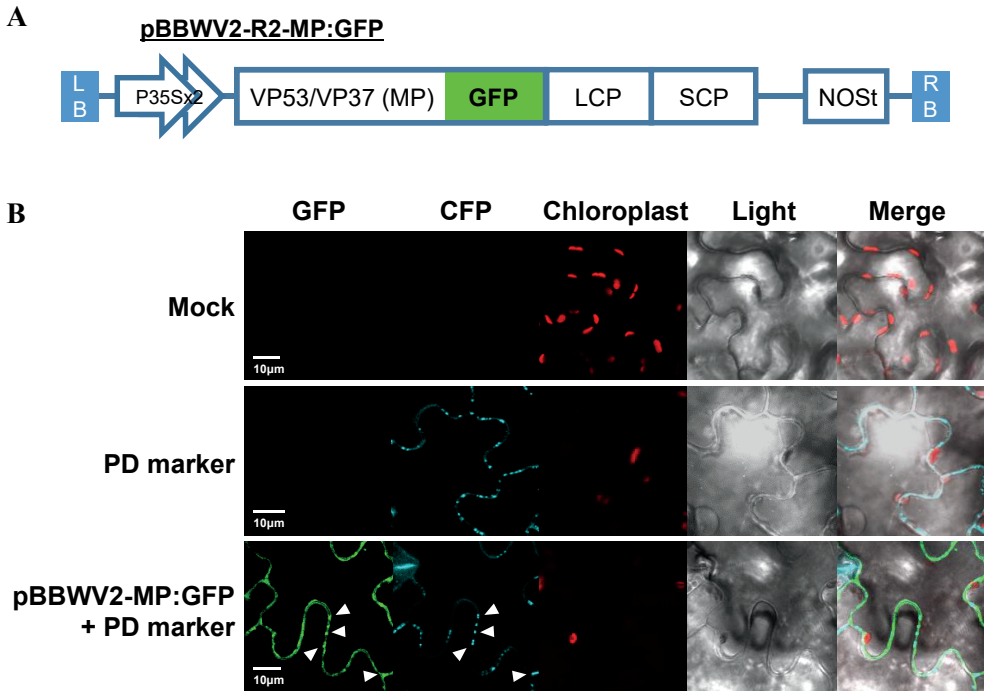


**Figure 1.** Subcellular localization of BBWV2-MP during viral infection. (A) Schematic representation of the construction of the pBBWV2-GFP. The binary vector contains a left border of T-DNA (LB), a double 35S promoter (35S), a NOS terminator (Tnos), and a right border of T-DNA (RB) in sequential order. MP, Movement protein; F, Flag; LCP, Large coat protein; SCP, Small coat protein. (B) Confocal images showing the subcellular distribution of GFP expressed by the BBWV2-GFP in *N. benthamiana* cells. Whole-leaf fluorescence signals were observed using an in vivo fluorescence imaging system. White arrowheads indicate areas where GFP is aggregated with PD marker.

## 2. Identification of host protein candidates interacting with BBWV2-MP

To investigate the host proteins that interact with BBWV2 viral protein MP, co-IP, and LC-MS/MS analysis were performed. Control (Healthy and pBBWV2-PAP1-R1 + pBBWV2-PAP1-R2-MP-B2), Flag (F) fusion BBWV2-MP:F (pBBWV2-PAP1-R1 + pBBWV2-PAP1-R2-MP:F-B2) constructs were agroinfiltrated into *N. benthamiana* leaves ($OD_{600}$: 0.5) (Figure 2A). At 37 dpi, infiltrated leaf tissues were ground in protein extraction buffer followed by centrifugation to remove the cell debris, the supernatant was then incubated with anti-FLAG antibody-coupled magnetic agarose beads. Proteins were eluted from the FLAG beads. Western blot analysis was performed to validate the co-IP reactions and confirmed that BBWV2-MP:F was successfully pulled down with the FLAG-specific antibodies (Figure 2B). SDS-PAGE gel analysis was also performed on co-immunoprecipitated products. The 6 bands showing different patterns from BBWV2-MP:F compared with healthy and mock were excised from the SDS-PAGE gel for subtractive profiling (Figure 2C). Another pattern that emerged compared to the control group was changed by BBWV2-MP:F, and it is possible that the BBWV2-MP:F protein interacted with other host proteins to form a complex. We tried to identify the host protein that interacts with the MP in the gel in the complex on the gel and subjected it to LC-MS/MS analysis. The result showed that most of the proteins were identified in the form of a monomer, dimer, and trimmer of heat shock protein 90-2 (Hsp90-2), and in addition, ER-luminal-binding protein (BLP4), Actin were identified with high MASCOT scores (Figure 2D).

**A**

**pBBWV2-PAP1-R1**

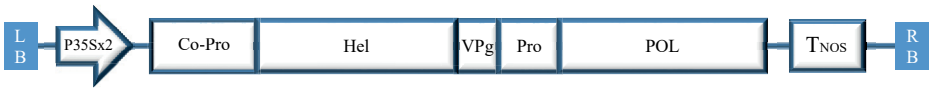


**pBBWV2-PAP1-R2-MP-B2**

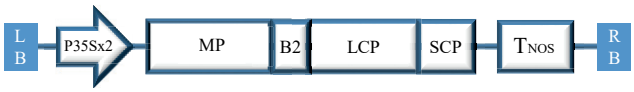


**pBBWV2-PAP1-R2-MP:F-B2**

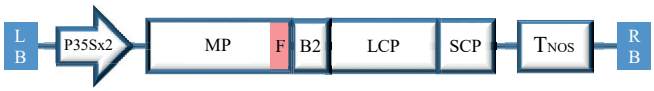


**B**

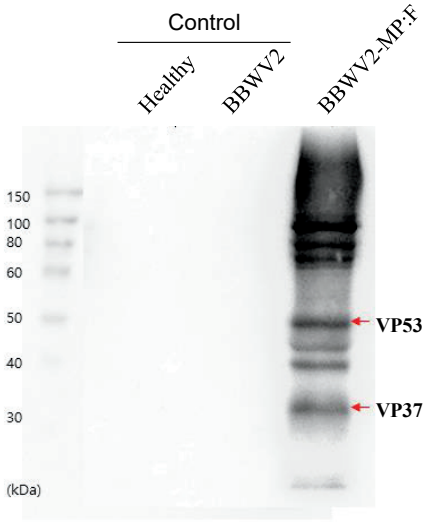


IP: Flag-IgG
IB: Flag-IgG, 5 msec. exposed

**C**

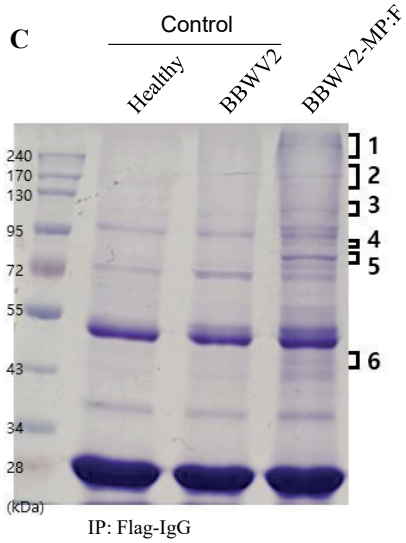


IP: Flag-IgG
Commassie-blue staining

**D**

| | Protein | Mass |
|---|---|---|
| 1 | Hsp90-2 tetramer | 80430 |
| 2 | Hsp90-2 dimer | 50420 |
| 3 | Unidentified | 42945 |
| 4 | Hsp90-2 monomer | 80430 |
| 5 | ER-luminal-binding protein (BLP4) | 73671 |
| 6 | Actin, GAPDH-A | 37620 |

**Figure 2.** Identification of host protein candidates interacting with BBWV2-MP. (A**)** Schematic representation of the construction of the pBBWV2. The binary vector contains a left border of T-DNA (LB), a double 35S promoter (35S), a NOS terminator (Tnos), and a right border of T-DNA (RB) in sequential order. Co-Pro, Protease cofactor; Hel, Helicase; VPg, Viral protein genome-linked; Pro, Protease; Pol, RNA-dependent RNA polymerase; MP, Movement protein; F, Flag; LCP, Large coat protein; SCP, Small coat protein. (B) Western blot and (C) SDS-PAGE gel analysis were performed with co-immunoprecipitated products. For subtractive profiling, The bands showing pattern differences from Healthy and BBWV2 lanes by fusion with Flag except for the position of the viral protein indicated by the red arrow in B were excised from the gel in BBWV2-MP:F lanes. Healthy, Non-infected; Mock, pBBWV2-PAP1-R1 + pBBWV2-PAP1-R2-MP-B2; BBWV2-MP:F, pBBWV2-PAP1-R1 + pBBWV2-PAP1-R2-MP:F-B2. RNA1 and RNA2 mixed equal proportions. (D) List of candidate proteins identified by LC-MS/MS. The candidate gene indicated by the number was extracted from the band of the number in C.

### 3. Identification of the interactions between BBWV2 VP37 and the components of the heat shock protein complex

Y2H screening system was performed in several steps in various combinations to determine whether the protein resulting from BBWV2-MP and LC-MS/MS and several other candidate genes directly interacted. The double-out selection medium means that the transformation was successful, the triple-out selection medium means the interaction of the two proteins, and the quadruple-out selection medium indicates the strong interaction of the two proteins. In the X-α-Gal assay, when the color of the colony turns blue, it indicates that the two proteins interact. The first step of the Y2H screening system was performed with various combinations for two viral components (VP37, VP53) to Hsp90-2, from LC-MS/MS results and heat shock protein 90-1 (Hsp90-1), heat shock protein 90-3 (Hsp90-3), which are the heat shock protein 90 (Hsp90) families of the same *N. benthamiana* and heat shock protein 70 (Hsp70) and Hsp70-Hsp90 organizing protein 3 (HOP3), which is known to complex of Hsp90 (Shirasu 2009; Xu et al. 2012). The data showed that all of the proteins transformed in the GBKT7 vector did not interact with the empty GADT7 vector (EV), indicating that there was no auto-activation activity (Figure 3, Table 8). And, only VP37 of the BBWV2 interacted with the Hsp90 family and HOP3 of *N. benthamiana* (Figure 3 and Table 8).

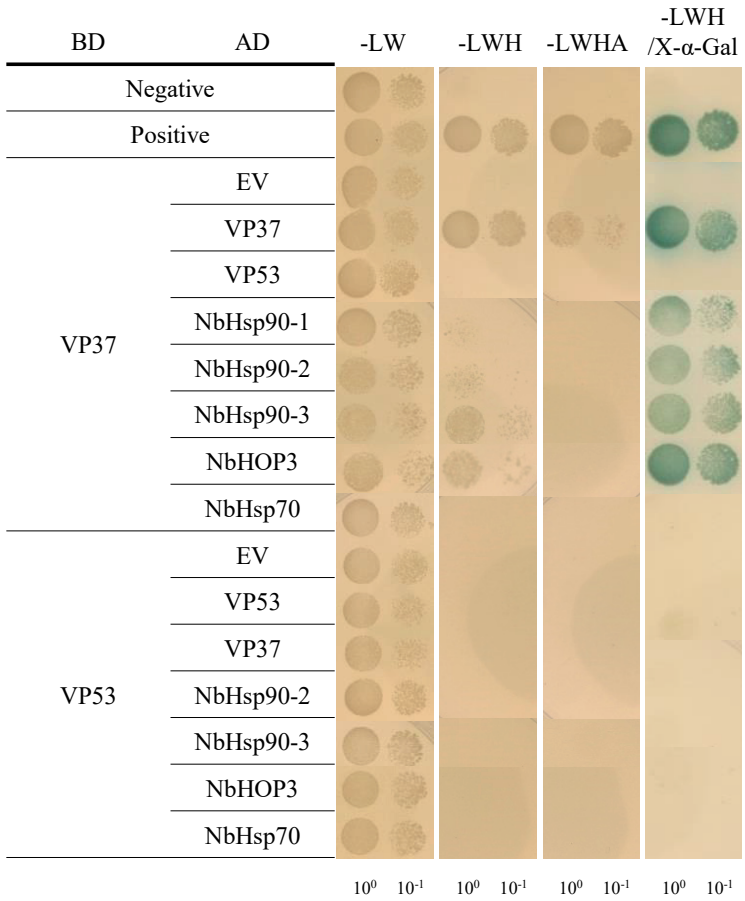


**Figure 3.** Yeast two-hybrid assay for identification of the interactions between the heat shock protein complex components and either BBWV2 VP37 or VP53. Full length of VP37, VP53 were cloned into the GAL4 DNA binding domain (BD) of pGBKT7. Full length of VP37, VP53, NbHsp90s, NbHOP3, NbHsp70 were cloned into the GAL4 DNA activation domain (AD) of pGADT7. Each of the genes was co-transformed into yeast cells (AH109) respectively, and cell growth on SD-based lack of selective medium (-LW, -LWH, -LWHA, -LWH/X-α-Gal). Ten-fold serial dilution of the transformants was plated on a selection medium. Cultivated for 3-5 days at 28°C. Positive interaction is indicated by growing colonies in –LWH and blue colonies in X-α-Gal, strong interaction is indicated by growing colonies in –LWHA. EV, Empty vector.

**Table 8.** Interaction mapping of the heat shock protein complex components and either BBWV2 VP37 or VP53

| | | BD | |
|---|---|---|---|
| | | VP37 | VP53 |
| AD | Empty | - | - |
| | VP37 | ++ | - |
| | VP53 | - | - |
| | NbHsp90-1 | + | ND* |
| | NbHsp90-2 | + | - |
| | NbHsp90-3 | + | - |
| | NbHOP3 | + | - |
| | NbHsp70 | - | - |

*ND: Not determined

## 4. The N-terminus of Hsp90-2 is crucial for interaction with VP37

A Y2H screening system was performed using an NbHsp90-2 truncated clone to identify important domains for the interaction between VP37 and NbHsp90-2. NbHsp90-2 is classified into N, M, C three substrate binding domains and charged linker (Figure 4B) (Ali et al. 2006; Xu et al. 2012). We tried to identify the interaction sites by deleting half of the N and C domains, and gradually narrowing the predicted interact site. As the data showed that ΔhC:NbHsp90-2 interacted, but ΔhN:NbHsp90-2 did not interact, and ΔhNC:NbHsp90-2 also did not interact (Figure 4A, 4C). Since the N domain was considered to be more important for interaction, the deleted N domain portion was gradually expanded. Neither NbHsp90-$2^{51\text{-}700}$ nor NbHsp90-$2^{26\text{-}700}$ appeared to interact, the amino acids 1 to 25 appear to play a decisive region in the interaction with VP37 (Figure 4).

**A**

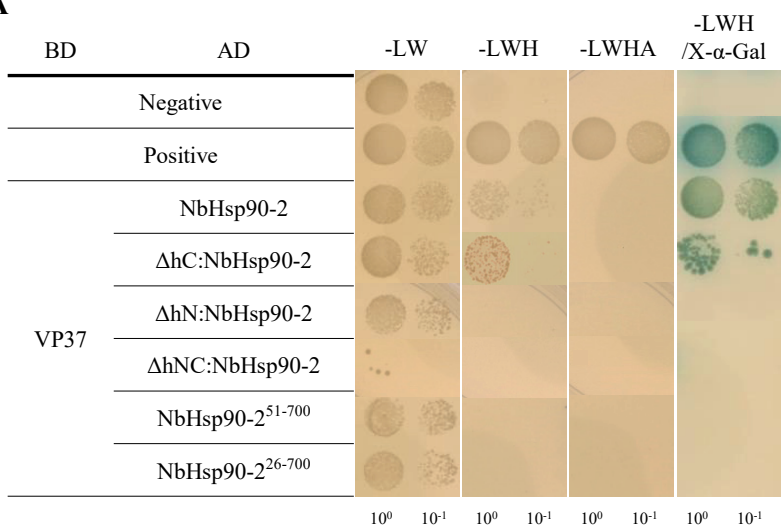


**B**

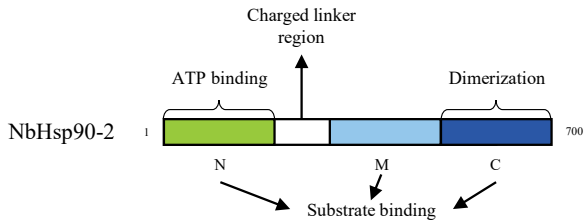


**C**

| Test clone | Amino acid position | Interaction with VP37 |
|---|---|---|
| ΔhC:NbHsp90-2 | 1 - 600 | + |
| ΔhN:NbHsp90-2 | 100 - 700 | - |
| ΔhNC:NbHsp90-2 | 100 - 600 | - |
| NbHsp90-2$^{51-700}$ | 51 - 700 | - |
| NbHsp90-2$^{26-700}$ | 26 - 700 | - |

1 MAEAETFAFQAEINQLLSLIINTFY 25

-: No interaction, +: Interaction

**Figure 4**. Yeast two-hybrid assay for identification of crucial domains of Hsp90 required for interaction with VP37. (A) VP37 was cloned into the GAL4 DNA binding domain (BD) of pGBKT7. NbHsp90-2 mutants were cloned into the GAL4 DNA activation domain (AD) of pGADT7. Each of the genes was co-transformed into yeast cells (AH109) respectively and cell growth on SD-based lack of selective medium (-LW, -LWH, -LWHA, -LWH/X-α-Gal). Ten-fold serial dilution of the transformants was plated on a selection medium. Cultivated for 3-5 days at 28°C. Positive interaction is indicated by growing colonies in –LWH and blue colonies in X-α-Gal, strong interaction is indicated by growing colonies in –LWHA. (B) Structural model of Hsp90. Hsp90 consists of three domains. N-terminal ATP-binding domain [N], A middle domain [M], A C-terminal dimerization [C], A charged region exists between the N and M domains. All domains reported interacting with different substrates. (C) Schematic representation and Amino acid position, degree of interaction. The N and C domains were deleted in half, and gradually recovering the deleted parts. Amino acid sequences from 1 to 25 are indicated on the NbHsp90-$2^{26\text{-}700}$, and negatively charged amino acids are indicated in red.

## 5. The charged amino acids at the N-terminus of Hsp90 is critical for interaction with VP37

Charged or polarized groups of amino acids have the property of electrostatic interactions. The regulation of these amino acid charges is known to have important influences such as reactions such as protein interaction and switching of signaling networks (Zhou and Pang 2018). We tried to determine whether three negatively charged Glu among 25 amino acids of NbHsp90-2 N-terminus influence the interaction with VP37. The three Glu were substituted with the non-charged amino acid Ala, either singly or in combination (Figure 5). The data show that E3A did not affect the interaction, and E5A or E12A did not interact alone or together (Figure 5). It can be seen that $E^{5}$ and $E^{12}$ of NbHsp90-2 were crucial in their interaction with VP37. And E5D and E12D substitute Glu to Asp, an amino acid with the same negative charge maintain the interaction alone or in combination, it was once again demonstrated that the charge of the amino acid influences the interaction between NbHsp90-2 and VP37 (Figure 5).

**A**

| BD | AD |
|---|---|
| Negative | |
| Positive | |
| VP37 | NbHsp90-2 |
| | NbHsp90-2$^{E3A}$ |
| | NbHsp90-2$^{E5A}$ |
| | NbHsp90-2$^{E12A}$ |
| | NbHsp90-2$^{E5,12A}$ |
| | NbHsp90-2$^{E3D}$ |
| | NbHsp90-2$^{E12D}$ |
| | NbHsp90-2$^{E5,12D}$ |

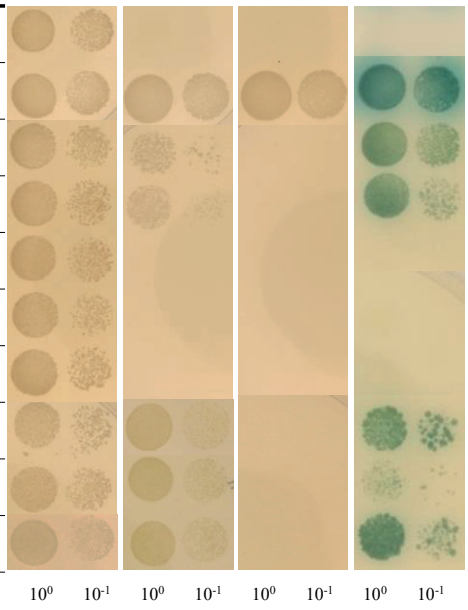


**B**

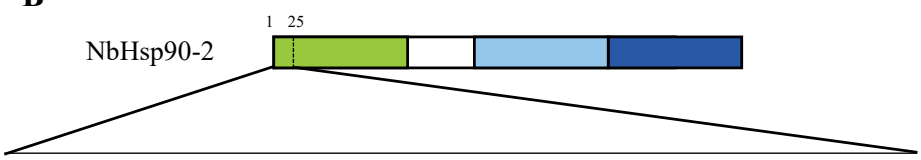


| Test clone | | Interaction with VP37 |
|---|---|---|
| NbHsp90-2 | MAEAETFAFQAEINQLLSLIINTFY··· | + |
| NbHsp90-2$^{E3A}$ | MA**A**AETFAFQAEINQLLSLIINTFY··· | + |
| NbHsp90-2$^{E5A}$ | MAEA**A**TFAFQAEINQLLSLIINTFY··· | - |
| NbHsp90-2$^{E12A}$ | MAEAETFAFQA**A**INQLLSLIINTFY··· | - |
| NbHsp90-2$^{E5,12A}$ | MAEA**A**TFAFQA**A**INQLLSLIINTFY··· | - |
| NbHsp90-2$^{E3D}$ | MA**D**AETFAFQAEINQLLSLIINTFY··· | + |
| NbHsp90-2$^{E12D}$ | MAEAETFAFQA**D**INQLLSLIINTFY··· | + |
| NbHsp90-2$^{E5,12D}$ | MAEA**D**TFAFQA**D**INQLLSLIINTFY··· | + |

-: No interaction, +: Interaction

**Figure 5**. Yeast two-hybrid assay for identification of crucial amino acids of Hsp90 in interaction with VP37. (A) VP37 was cloned into the GAL4 DNA binding domain (BD) of pGBKT7. Amino acid substituted NbHsp90-2 mutants were cloned into the GAL4 DNA activation domain (AD) of pGADT7 respectively. Each of the genes was co-transformed into yeast cells (AH109) and cell growth on SD-based lack of selective medium (-LW, -LWH, -LWHA, -LWH/X-α-Gal). Ten-fold serial dilution of the transformants was plated on a selection medium. Cultivated for 3-5 days at 28°C. Positive interaction is indicated by growing colonies in –LWH and blue colonies in X-α-Gal, strong interaction is indicated by growing colonies in –LWHA. (B) Schematic representation of amino acid substituted NbHsp90-2 clone and indicate substituted position, degree of interaction. Substitute amino acids are indicated in red.

## 6. Identification of crucial domains of VP37 required for interaction with Hsp90

In the interaction between VP37 and NbHsp90-2, to identify the critical domain of VP37, eliminate 1/3 from the N-terminus and C-terminus of VP37, and Y2H screening was performed while gradually recovering the truncated region. The data show that $VP37^{31-337}$ interacts, so the amino acids from 31 to 43 in VP37 appear to be important for the interaction with NbHsp90-2 (Figure 6). In NbHsp90-2, negatively charged amino acids were crucial (Figure 5), so at first, we thought that positively charged amino acids in $VP37^{31-337}$ would be important for interaction.

The amino acid substitution was performed to determine whether the amino acids charged in VP37 influence the interaction. The result of the substitution of positively charged amino acids in $VP37^{31-337}$ to Ala does not appear to interact, so positively charged amino acids appear to be critical amino acids for interaction (Figure 7A, 7B). However, substitutions of positively charged amino acid to alanine in full-length VP37 did not appear to affect the interaction with NbHsp90-2 (Figure 7A, 7B). Additionally, the substitution of negatively charged amino acids to alanine also did not interact with NbHsp90-2 (Figure 7A, 7B). As a result, $VP37^{31-43}$ region didn't affect the interaction with NbHsp90-2. Further, we investigate $VP37^{1-326}$, which narrowed the truncated region, and the results show that both constructs interact with NbHsp90-2 (Figure 6A, 6B), so amino acids 309 to 326 of VP37 seem to be more crucial for the interaction (Figure 7C).

**A**

| BD | AD |
|---|---|
| Negative | |
| Positive | |
| VP37 | NbHsp90-2 |
| Δ1/3C:VP37 | |
| Δ1/3N:VP37 | |
| Δ1/6C:VP37 | |
| Δ1/6N:VP37 | |
| $VP37^{1-308}$ | |
| $VP37^{31-337}$ | |
| $VP37^{44-337}$ | |
| $VP37^{1-326}$ | |
| $VP37^{16-337}$ | |

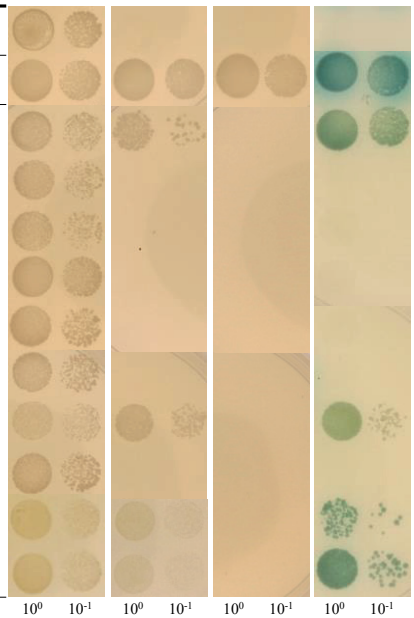


**B**

| Test clone | Amino acid position | Interaction with VP37 |
|---|---|---|
| Δ1/3C:VP37 | 1 - 225 | - |
| Δ1/6C:VP37 | 1 - 281 | - |
| $VP37^{1-308}$ | 1 - 308 | - |
| $VP37^{1-326}$ | 1 - 326 | + |
| Δ1/3N:VP37 | 112 -337 | - |
| Δ1/6N:VP37 | 56 - 337 | - |
| $VP37^{44-337}$ | 44 - 337 | - |
| $VP37^{31-337}$ | 31 - 337 | + |

-: No interaction, +: Interaction

**Figure 6.** Yeast two-hybrid assay for identification of crucial domains of VP37 required for interaction with Hsp90. (A) Truncated VP37 mutants were cloned into the GAL4 DNA binding domain (BD) of pGBKT7. NbHsp90-2 was cloned into the GAL4 DNA activation domain (AD) of pGADT7. Each of the genes was co-transformed into yeast cells (AH109) and cell growth on SD-based lack of selective medium (-LW, -LWH, -LWHA, -LWH/X-α-Gal). Ten-fold serial dilution of the transformants was plated on a selection medium. Cultivated for 3-5 days at 28°C. Positive interaction is indicated by growing colonies in –LWH and blue colonies in X-α-Gal, strong interaction is indicated by growing colonies in –LWHA. (B) Schematic representation and truncated amino acid position, degree of interaction. Delete 1/3 from the N-terminal or C-terminal, and gradually recovering the deleted parts.

**A**

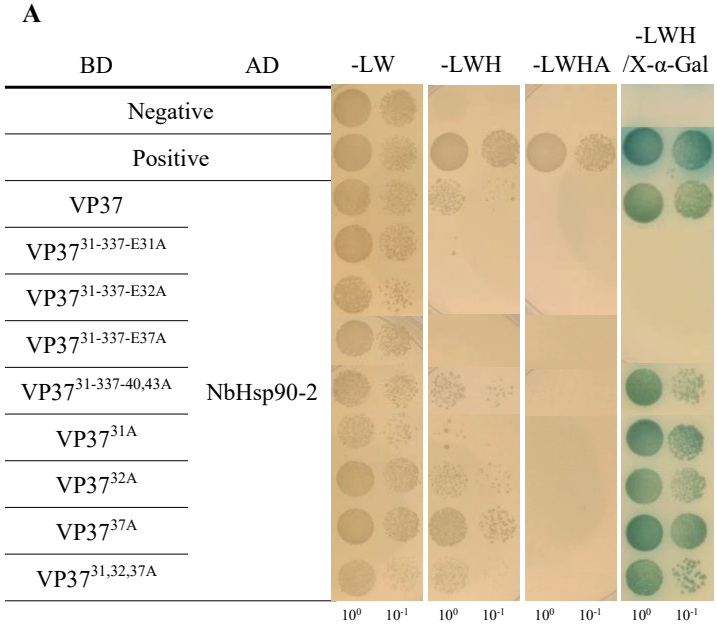


**B**

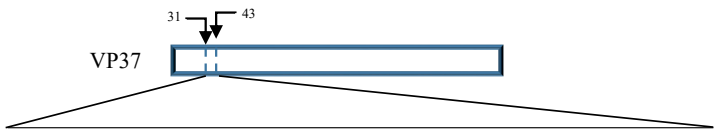


| Test clone | | Interaction with NbHsp90-2 |
|---|---|---|
| VP37 | ⋯KKSILPRVQDLYE⋯ | + |
| VP37$^{31\text{-}337\text{-}31A}$ | AKSILPRVQDLYE⋯ | - |
| VP37$^{31\text{-}337\text{-}32A}$ | KASILPRVQDLYE⋯ | - |
| VP37$^{31\text{-}337\text{-}37A}$ | KKSILPAVQDLYE⋯ | - |
| VP37$^{31\text{-}337\text{-}40,\ 43A}$ | KKSILPRVQALYA⋯ | + |
| VP37$^{31A}$ | ⋯AKSILPRVQDLYE⋯ | + |
| VP37$^{32A}$ | ⋯KASILPRVQDLYE⋯ | + |
| VP37$^{37A}$ | ⋯KKSILPAVQDLYE⋯ | + |
| VP37$^{31,32,37A}$ | ⋯AASILPAVQDLYE⋯ | + |

-: No interaction, +: Interaction

**C**

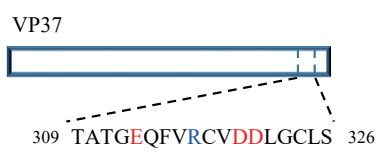

**Figure 7.** Yeast two-hybrid assay for identification of crucial amino acids of VP37 in interaction with Hsp90. (A) Substituted VP37 mutants were cloned into the GAL4 DNA binding domain (BD) of pGBKT7 respectively. NbHsp90-2 was cloned into the GAL4 DNA activation domain (AD) of pGADT7. Each of the genes was co-transformed into yeast cells (AH109) and cell growth on SD-based lack of selective medium (-LW, -LWH, -LWHA, -LWH/X-α-Gal). Ten-fold serial dilution of the transformants was plated on a selection medium. Cultivated for 3-5 days at 28°C. Positive interaction is indicated by growing colonies in –LWH and blue colonies in X-α-Gal, strong interaction is indicated by growing colonies in –LWHA. (B) Schematic representation of substituted amino acid position, degree of interaction. Substitute amino acids are marked in red. (C) Schematic representation of VP37 shows the amino acid sequence from 309 to 326. Positively charged amino acids are indicated in blue and negative charged amino acids are indicated in red.

# DISCUSSION

To successfully establish an infection, viruses modify the host cell environment through various mechanisms to impair cellular function and optimize viral replication (Garcia and Pallas 2015; Villanueva et al. 2005). In the virus, the interaction with the host is one of the very important parts in the movement of the virus in vivo, and it has been reported that many host proteins interact with the viral MP (Chen et al. 2000; Kaido et al. 2007; Link and Sonnewald 2016; Uhrig and MacFarlane 2008). In this paper, we found evidence that VP37, an MP of BBWV2, directly interacts with Hsp90-2 of *N. benthamiana*, which is likely to be involved in the movement of BBWV2.

The protein chaperones of the heat shock protein 40, 70, 90, and 100 (Hsp40, Hsp70, Hsp90, and Hsp100) family are highly conserved throughout eukaryotes and are essential for the quality control of cellular proteins and protein complexes that contribute to a wide range of cellular processes (Mayer 2010). In the context of cell quality control machinery, chaperones maintain homeostasis within the plant by refolding misfolded or aggregated proteins or causing them to break down (Bukau et al. 2006; Tyedmers et al. 2010). The cytosolic Hsp70 family can interact with a variety of cofactors and folding substrates and contribute to a variety of biological processes and play an important role in the replication cycle, intercellular transport, and virion assembly of many positive-stranded RNA viruses, including *Potexvirus*, *Tobamovirus*, *Potyvirus*, *Cucumovirus*, *Tombusvirus*, *Carmovirus* (Chen et al. 2008; Kampinga and Craig 2010; Mathioudakis et al. 2012; Verchot 2012; Wang et al. 2009). Even, the viral MP of *Closterovirus* is an Hsp70 homolog that functions to both stabilize the tail region of the virion and aid trafficking across PD (Alzhanova et al. 2007; Satyanarayana et al. 2004; Satyanarayana et al. 2000; Tatineni et al. 2010). Hsp90 is a highly conserved eukaryotic

molecular chaperone. It contributes to the stabilization or activation of proteins involved in signaling, protein trafficking, and immunity. Hsp90 generally forms dimers, and, like Hsp70, its association with client proteins is regulated by ATP binding and hydrolysis, as well as co-chaperones (Verchot 2012). Hsp90 plays a positive role in infection with bamboo mosaic virus (BaMV, *Potexvirus*), red clover necrotic mosaic virus (RCNMV, *Dianthovirus*), and feline herpes virus (FHV, *Varicellovirus*), and these have been reported to promote replication by forming partnerships with various viral replicase (Huang et al. 2012; Kampmueller and Miller 2005; Mine et al. 2012; Mine et al. 2010). As such, Hsp70 can be considered to be recruited and contributed to the replication, intercellular transport, and recombination of various viral species. Each virus has different characteristics, so there seems to be no commonality between hsp90 and its replicase. However, from the function of Hsp90, it can be seen that Hsp90 is involved in other processes after being recruited by recognizing the characteristic fold part of the virus (Huang et al. 2012). It has been known that only Hsp70 contributes to intercellular transport, and most of Hsp90 contributes to viral replication.

In the BBWV2*,* genus *Fabavirus,* family *Secoviridae*, there has been no investigation on the host protein that interacts with MP, and our results show that Hsp90-2 directly interacts with the VP37, an MP of BBWV2 (Figure 3). Especially in the negative charged amino acids E5, E12 located in the N-domain of Hsp90-2 is crucial for the interaction (Figure 5). Even VP53 has all the sequences of VP37, but no interaction was found (Figure 3). This suggests that the two are proteins that share a sequence but function completely differently. And this can be seen as evidence that Hsp90-2 recognizes the VP37, as a client protein and is directly involved in the movement of BBWV2. And Hsp90 appears to have a different function in its interaction with BBWV2 than in other viruses. Hsp90 formed a replication complex as mentioned above in other viruses, suggesting that it is important for replication. However, our

findings appear to be related to the intracellular transport of Hsp90 through interactions with movement protein

Host proteins that Hsp90 interacts with are known to have TPR domains. Among the TPR domain proteins to which hsp90 binds, the prominent one is the high molecular weight immunophilin. Immunophilins are known to be involved in intracellular transport (Pratt et al. 2004; Pratt et al. 2001). VP37 does not have a TPR domain and it is unclear how Hsp90 recognizes VP37. However, the results of the LC-MS/MS and the Y2H indicate that VP37 co-interacts with Hsp90 and HOP3, which has a TPR domain. Therefore, it can be suggested that the VP37 interacts directly with Hsp90, and localizes to PD using intracellular transport of host for infection.

We conducted experiments to identify host protein involved in the viral movement of BBWV2, and our results confirmed the interaction between VP37 and NbHsp90-2 in *N. benthamiana* and determined the sites of the interaction.

# REFERENCES

**Ali MMU, Roe SM, Vaughan CK, Meyer P, Panaretou B, Piper PW, Prodromou C, Pearl LH** (2006) Crystal structure of an Hsp90-nucleotide-p23/Sba1 closed chaperone complex. Nature 440 (7087):1013-1017. doi:10.1038/nature04716

**Alzhanova DV, Prokhnevsky AI, Peremyslov VV, Dolja VV** (2007) Virion tails of Beet yellows virus: Coordinated assembly by three structural proteins. Virology 359 (1):220-226. doi:10.1016/j.virol.2006.09.007

**Atkinson NJ, Urwin PE** (2012) The interaction of plant biotic and abiotic stresses: from genes to the field. J Exp Bot 63 (10):3523-3543. doi:10.1093/jxb/ers100

**Atsumi G, Tomita R, Kobayashi K, Sekine KT** (2013) Establishment of an agroinoculation system for broad bean wilt virus 2. Arch Virol 158 (7):1549-1554. doi:10.1007/s00705-013-1625-7

**Bukau B, Weissman J, Horwich A** (2006) Molecular chaperones and protein quality control. Cell 125 (3):443-451. doi:10.1016/j.cell.2006.04.014

**Carbonell A, García JA, Simón-Mateo C, Hernández C** (2016) Plant Virus RNA Replication. In: eLS. pp 1-13. doi:https://doi.org/10.1002/9780470015902.a0022338

**Chen MH, Sheng J, Hind G, Handa AK, Citovsky V** (2000) Interaction between the tobacco mosaic virus movement protein and host cell pectin methylesterases is required for viral cell-to-cell movement. The EMBO journal 19 (5):913-920. doi:10.1093/emboj/19.5.913

**Chen Z, Zhou T, Wu X, Hong Y, Fan Z, Li H** (2008) Influence of cytoplasmic heat shock protein 70 on viral infection of Nicotiana benthamiana. Mol Plant Pathol 9 (6):809-817. doi:10.1111/j.1364-3703.2008.00505.x

**Choi B, Kwon S-J, Kim M-H, Choe S, Kwak H-R, Kim M-K, Jung C, Seo J-K** (2019) A Plant Virus-Based Vector System for Gene Function Studies in Pepper. Plant Physiology 181 (3):867. doi:10.1104/pp.19.00836

**Ferrer RM, Ferriol I, Moreno P, Guerri J, Rubio L** (2011) Genetic variation and evolutionary analysis of broad bean wilt virus 2. Arch Virol 156 (8):1445-1450. doi:10.1007/s00705-011-0990-3

**Garcia JA, Pallas V** (2015) Viral factors involved in plant pathogenesis. Curr Opin Virol 11:21-30. doi:10.1016/j.coviro.2015.01.001

**Genovés A, Navarro JA, Pallás V** (2009) A self-interacting carmovirus movement protein plays a role in binding of viral RNA during the cell-to-cell movement and shows an actin cytoskeleton dependent location in cell periphery. Virology 395 (1):133-142. doi:10.1016/j.virol.2009.08.042

**Gietz RD, Woods RA** (2002) Transformation of yeast by lithium acetate/single-stranded carrier DNA/polyethylene glycol method. Methods Enzymol 350:87-96. doi:10.1016/s0076-6879(02)50957-5

**Huang YW, Hu CC, Liou MR, Chang BY, Tsai CH, Meng M, Lin NS, Hsu YH** (2012) Hsp90 interacts specifically with viral RNA and differentially regulates replication initiation of Bamboo mosaic virus and associated satellite RNA. PLoS Pathog 8 (5):e1002726. doi:10.1371/journal.ppat.1002726

**Kaido M, Inoue Y, Takeda Y, Sugiyama K, Takeda A, Mori M, Tamai A, Meshi T, Okuno T, Mise K** (2007) Downregulation of the NbNACa1 gene encoding a movement-protein-interacting protein reduces cell-to-cell movement of Brome mosaic virus in Nicotiana benthamiana. Mol Plant Microbe Interact 20 (6):671-681. doi:10.1094/mpmi-20-6-0671

**Kampinga HH, Craig EA** (2010) The HSP70 chaperone machinery: J proteins as drivers of functional specificity. Nat Rev Mol Cell Biol 11 (8):579-592. doi:10.1038/nrm2941

**Kampmueller KM, Miller DJ** (2005) The cellular chaperone heat shock protein 90 facilitates Flock House virus RNA replication in Drosophila cells. J Virol 79 (11):6827-6837. doi:10.1128/jvi.79.11.6827-6837.2005

**Kasteel DT, Perbal MC, Boyer JC, Wellink J, Goldbach RW, Maule AJ, van Lent JW** (1996) The movement proteins of cowpea mosaic virus and cauliflower mosaic virus induce tubular structures in plant and insect cells. J Gen Virol 77 ( Pt 11):2857-2864. doi:10.1099/0022-1317-77-11-2857

**Kong L, Wang Y, Yang X, Sunter G, Zhou X** (2014) Broad bean wilt virus 2 encoded VP53, VP37 and large capsid protein orchestrate suppression of RNA silencing in plant. Virus research 192:62-73. doi:10.1016/j.virusres.2014.08.010

**Kwak HR, Kim MK, Lee YJ, Seo JK, Kim JS, Kim KH, Cha B, Choi HS** (2013) Molecular Characterization and Variation of the Broad bean wilt virus 2 Isolates Based on Analyses of Complete Genome Sequences. Plant Pathol J 29 (4):397-409. doi:10.5423/PPJ.OA.03.2013.0036

**Link K, Sonnewald U** (2016) Interaction of Movement Proteins with Host Factors, Mechanism of Viral Host Cell Manipulation and Influence of MPs on Plant Growth and Development. In: Kleinow T (ed) Plant-Virus Interactions: Molecular Biology, Intra- and Intercellular Transport. Springer International Publishing, Cham, pp 1-37. doi:10.1007/978-3-319-25489-0_1

**Liu C, Meng C, Xie L, Hong J, Zhou X** (2009) Cell-to-cell trafficking, subcellular distribution, and binding to coat protein of Broad bean wilt virus 2 VP37 protein. Virus Res 143 (1):86-93. doi:10.1016/j.virusres.2009.03.009

**Liu C, Nelson RS** (2013) The cell biology of Tobacco mosaic virus replication and movement. Front Plant Sci 4:12. doi:10.3389/fpls.2013.00012

**Liu C, Ye L, Lang G, Zhang C, Hong J, Zhou X** (2011) The VP37 protein of Broad bean wilt virus 2 induces tubule-like structures in both plant and insect cells. Virus Research 155 (1):42-47. doi:https://doi.org/10.1016/j.virusres.2010.08.013

**Lucas WJ** (2006) Plant viral movement proteins: agents for cell-to-cell trafficking of viral genomes. Virology 344 (1):169-184. doi:10.1016/j.virol.2005.09.026

**Mathioudakis MM, Veiga R, Ghita M, Tsikou D, Medina V, Canto T, Makris AM, Livieratos IC** (2012) Pepino mosaic virus capsid protein interacts with a tomato heat shock protein cognate 70. Virus Res 163 (1):28-39. doi:10.1016/j.virusres.2011.08.007

**Mayer MP** (2010) Gymnastics of molecular chaperones. Mol Cell 39 (3):321-331. doi:10.1016/j.molcel.2010.07.012

**Mine A, Hyodo K, Tajima Y, Kusumanegara K, Taniguchi T, Kaido M, Mise K, Taniguchi H, Okuno T** (2012) Differential roles of Hsp70 and Hsp90 in the assembly of the replicase complex of a positive-strand RNA plant virus. J Virol 86 (22):12091-12104. doi:10.1128/jvi.01659-12

**Mine A, Takeda A, Taniguchi T, Taniguchi H, Kaido M, Mise K, Okuno T** (2010) Identification and characterization of the 480-kilodalton template-specific RNA-dependent RNA polymerase complex of red clover necrotic mosaic virus. Journal of virology 84 (12):6070-6081. doi:10.1128/JVI.00054-10

**Navarro JA, Sanchez-Navarro JA, Pallas V** (2019) Key checkpoints in the movement of plant viruses through the host. Adv Virus Res 104:1-64. doi:10.1016/bs.aivir.2019.05.001

**Nelson RS, Citovsky V** (2005) Plant Viruses. Invaders of Cells and Pirates of Cellular Pathways. Plant Physiology 138 (4):1809. doi:10.1104/pp.104.900167

**Niehl A, Heinlein M** (2011) Cellular pathways for viral transport through plasmodesmata. Protoplasma 248 (1):75-99. doi:10.1007/s00709-010-0246-1

**Osterbaan LJ, Fuchs M** (2019) Dynamic interactions between plant viruses and their hosts for symptom development. Journal of Plant Pathology 101 (4):885-895. doi:10.1007/s42161-019-00323-5

**Pallas V, Garcia JA** (2011) How do plant viruses induce disease? Interactions and interference with host components. J Gen Virol 92 (Pt 12):2691-2705. doi:10.1099/vir.0.034603-0

**Pratt WB, Galigniana MD, Harrell JM, DeFranco DB** (2004) Role of hsp90 and the hsp90-binding immunophilins in signalling protein movement. Cell Signal 16 (8):857-872. doi:10.1016/j.cellsig.2004.02.004

**Pratt WB, Krishna P, Olsen LJ** (2001) Hsp90-binding immunophilins in plants: the protein movers. Trends Plant Sci 6 (2):54-58. doi:10.1016/s1360-1385(00)01843-4

**Rejeb IB, Pastor V, Mauch-Mani B** (2014) Plant Responses to Simultaneous Biotic and Abiotic Stress: Molecular Mechanisms. Plants (Basel, Switzerland) 3 (4):458-475. doi:10.3390/plants3040458

**Ritzenthaler C, Hofmann C** (2007) Tubule-guided movement of plant viruses In Viral Transport in Plants (Waigmann E., editor; and Heinlein M., editor., eds), vol 7. Viral Transport in Plants. Heidelberg, Berlin: Springer-Verlag.[Google Scholar], Viral Transport in Plants. doi:https://doi.org/10.1007/7089_2006_105

**Satyanarayana T, Gowda S, Ayllón MA, Dawson WO** (2004) Closterovirus bipolar virion: evidence for initiation of assembly by minor coat protein and its restriction to the genomic RNA 5' region. Proc Natl Acad Sci U S A 101 (3):799-804. doi:10.1073/pnas.0307747100

**Satyanarayana T, Gowda S, Mawassi M, Albiach-Martí MR, Ayllón MA, Robertson C, Garnsey SM, Dawson WO** (2000) Closterovirus encoded HSP70 homolog and p61 in addition to both coat proteins function in efficient virion assembly. Virology 278 (1):253-265. doi:10.1006/viro.2000.0638

**Seo J-K, Kim K-H** (2016) Long-Distance Movement of Viruses in Plants. In: Current Research Topics in Plant Virology. Springer, pp 153-172

**Shirasu K** (2009) The HSP90-SGT1 chaperone complex for NLR immune sensors. Annu Rev Plant Biol 60:139-164. doi:10.1146/annurev.arplant.59.032607.092906

**Suzuki N, Rivero RM, Shulaev V, Blumwald E, Mittler R** (2014) Abiotic and biotic stress combinations. New Phytol 203 (1):32-43. doi:10.1111/nph.12797

**Syller J, Grupa A** (2016) Antagonistic within-host interactions between plant viruses: molecular basis and impact on viral and host fitness. Mol Plant Pathol 17 (5):769-782. doi:10.1111/mpp.12322

**Tanaka K, Choi J, Cao Y, Stacey G** (2014) Extracellular ATP acts as a damage-associated molecular pattern (DAMP) signal in plants. Front Plant Sci 5:446. doi:10.3389/fpls.2014.00446

**Tatineni S, Gowda S, Dawson WO** (2010) Heterologous minor coat proteins of Citrus tristeza virus strains affect encapsidation, but the coexpression of HSP70h and p61 restores encapsidation to wild-type levels. Virology 402 (2):262-270. doi:10.1016/j.virol.2010.03.042

**Tyedmers J, Mogk A, Bukau B** (2010) Cellular strategies for controlling protein aggregation. Nat Rev Mol Cell Biol 11 (11):777-788. doi:10.1038/nrm2993

**Uhrig JF, MacFarlane SA** (2008) Protein-Protein Interactions in Plant Virus Movement and Pathogenicity. In: Nautiyal CS, Dion P (eds) Molecular Mechanisms of Plant and Microbe Coexistence. Springer Berlin Heidelberg, Berlin, Heidelberg, pp 319-338. doi:10.1007/978-3-540-75575-3_13

**Verchot J** (2012) Cellular chaperones and folding enzymes are vital contributors to membrane bound replication and movement complexes during plant RNA virus infection. Front Plant Sci 3:275. doi:10.3389/fpls.2012.00275

**Villanueva RA, Rouillé Y, Dubuisson J** (2005) Interactions between virus proteins and host cell membranes during the viral life cycle. Int Rev Cytol 245:171-244. doi:10.1016/s0074-7696(05)45006-8

**Waigmann E, Ueki S, Trutnyeva K, Citovsky V** (2004) The Ins and Outs of Nondestructive Cell-to-Cell and Systemic Movement of Plant Viruses. Critical Reviews in Plant Sciences 23 (3):195-250. doi:10.1080/07352680490452807

**Wang L, Tan H, Wu M, Jimenez-Gongora T, Tan L, Lozano-Duran R** (2017) Dynamic Virus-Dependent Subnuclear Localization of the Capsid Protein from a Geminivirus. Frontiers in plant science 8:2165-2165. doi:10.3389/fpls.2017.02165

**Wang RY, Stork J, Nagy PD** (2009) A key role for heat shock protein 70 in the localization and insertion of tombusvirus replication proteins to intracellular membranes. J Virol 83 (7):3276-3287. doi:10.1128/jvi.02313-08

**Wellink J, van Lent JW, Verver J, Sijen T, Goldbach RW, van Kammen A** (1993) The cowpea mosaic virus M RNA-encoded 48-kilodalton protein is responsible for induction of tubular structures in protoplasts. J Virol 67 (6):3660-3664. doi:10.1128/jvi.67.6.3660-3664.1993

**Xie L, Shang W, Liu C, Zhang Q, Sunter G, Hong J, Zhou X** (2016) Mutual association of Broad bean wilt virus 2 VP37-derived tubules and plasmodesmata obtained from cytological observation. Sci Rep 6:21552. doi:10.1038/srep21552

**Xu ZS, Li ZY, Chen Y, Chen M, Li LC, Ma YZ** (2012) Heat shock protein 90 in plants: molecular mechanisms and roles in stress responses. Int J Mol Sci 13 (12):15706-15723. doi:10.3390/ijms131215706

**Zhou H-X, Pang X** (2018) Electrostatic Interactions in Protein Structure, Folding, Binding, and Condensation. Chemical reviews 118 (4):1691-1741. doi:10.1021/acs.chemrev.7b00305

# ABSTRACT IN KOREAN

## 잠두위조바이러스 2 와 기주 간의 병원성 및 분자적 상호작용에 대한 특성 구명

김명휘

서울대학교 국제농업기술대학원 국제농업기술학전공

지도교수 서장균

Broad bean wilt virus 2 (BBWV2; *Fabavirus* 속, *Secoviridae* 과)는 광범위한 숙주 범위를 가지고 전세계적으로 확산된 진화적으로 체계를 잘 갖춘 RNA 바이러스이다. 다양한 식물에서 많은 BBWV2 분리주가 확인되었지만, 게놈 서열과 관련된 병원성 및 증상 특성 또는, 숙주 단백질과의 상호 작용에 대한 분자 특성에 대한 정보는 거의 없다. 따라서, 본 연구에서 우리는 서로 다른 기주에서 각각 얻은 BBWV2-PC, -LS2 및 P3 의 세 가지 유 전적으로 멀리 떨어져있는 BBWV2 분리주의 분자 및 병원성 특성에 대한 통합 정보와 바이러스와 상호작용하여 바이러스의 이동에 관여할 것으로 보이는 기주 단백질에 대해 구명하였다. 다양한 숙주에서 분리된 42 개의 BBWV2 분리주 집단의 계통 발생 및 다양성 분석은 RNA2 가 RNA1 보다 더 높은 유전적 유연성을 가지며 숙주가

부과한 제약 하에서 진화했을 수 있음을 보여주었다. 또한, BBWV2-PC RNA2 의 감염성 cDNA 클론을 이용한 pseudo-recombinant 병원성 분석은 RNA2 가 BBWV2 의 병원성과 관련된 바이러스 인자(들)를 포함한다는 것을 입증했다. 식물 바이러스는 절대 기생체로 게놈 복제, 세포 및 전신 이동 등, 기주 안에서 기주를 통해 모든 생활 주기를 영위해 나가며, 이를 위해 다양한 기주 인자를 필요로 한다. 그 중 세포 내 바이러스의 이동은 원형질 연락사를 통해 감염된 세포에서 인접된 세포로 일어나며, 이 과정에서 바이러스의 이동단백질은 바이러스 단백질을 원형질 연락사로 국소화 시키기 위해 기주 단백질과의 상호 작용이 필수적이다. BBWV2 는 RNA2 에 암호화 된 VP37 이 이동 단백질로 작용한다고 알려져 있다. 공동 면역침강기법을 통해 VP37 과 상호 작용하는 후보 숙주 인자로 열충격단백질 90 (Hsp90)을 확인했다. Hsp90 은 다양한 생물학적 과정에서 여러 공동 샤페론과 상호 작용하여 식물의 유전적 항상성을 유지하는 분자 보호자 중 하나이다. 효모단백질잡종법 (Y2H)을 사용하여, VP37 과 Hsp90 간의 직접적인 상호 작용을 입증하였고, Y2H 를 기반으로 VP37/Hsp90 상호 작용을 추가로 분석하여 상호 작용에 대한 중요한 모티프와 아미노산 잔기를 식별했다. 그 결과, VP37 과의 상호 작용에는 Hsp90 N-말단 영역의 두 개의 아미노산 잔기 (E5 및 E12)가 결정적인 것을 확인했다. 따라서 우리의 연구는 RNA2 와 그 암호화 된 단백질이 바이러스의 병원성 및 생물학적 특성을 결정하는 BBWV2-기주 상호 작용과 밀접하게 관련되어 있음을 시사한다.

주요어: 잠두위조바이러스 2, 집단 다양성 분석, 병원성, 기주-바이러스 상호작용, 단백질-단백질 상호작용

학번: 2019-27060

# 감사의 글

우선 논문을 완성하기에 도움을 주신 많은 분들에게 감사의 인사를 전합니다. 아무것도 없이 평창으로 올라와 학교에 입학하기까지 부족한 저를 믿고 받아주시고 많은 지도와 아낌없는 지원을 해주신 서장균 교수님께 많은 감사의 인사를 드립니다. 그리고 여러 분야의 다양한 관점에서 여러 가르침과 조언을 해주신 김주곤 교수님, 강진호 교수님, 정춘균 교수님께도 감사의 인사를 드립니다.

평창에서 보다 긴 시간을 있게 되었지만, 함께 지내고 여러 일을 하며 많은 도움을 준 실험실 식구들과, 함께 웃고 즐기며 서로의 일을 함께한 작물유전체육종 연구실, 작물분자생물학 연구실 모두에게도 감사합니다.

마지막으로 집 떠나 멀리 나온 아들에게 묵묵히 계속해서 지원해준 가족 모두에게 감사하고 앞으로도 더 열심히 해나가겠습니다. 그리고 기쁘거나 힘들 때 서로 의지하고 지냈던 친구들 모두 고맙습니다.

석사학위 기간 동안 훌륭한 교수님들과 좋은 사람들을 만나 좋은 시간을 보내었고, 앞으로도 계속해서 더 좋은 모습으로 보답하도록 하겠습니다.